Open access • Journal Article • DOI:10.1039/C7MH01139C

Biofabrication of multifunctional nanocellulosic 3D structures: A facile and customizable route — Source link

Luiz G. Greca, Janika Lehtonen, Blaise L. Tardy, Jiaqi Guo ...+1 more authors

Institutions: Aalto University

Published on: 08 May 2018 - Materials horizons (The Royal Society of Chemistry)

Topics: Biofabrication

Department of Bioproducts and Biosystems

Functional Materials from Nanocellulosic Networks and Uses in Water Purification

Janika Lehtonen

Aalto University

DOCTORAL DISSERTATIONS

Aalto University publication series
DOCTORAL DISSERTATIONS 218/2020

Functional Materials from Nanocellulosic Networks and Uses in Water Purification

Janika Lehtonen

A doctoral dissertation completed for the degree of Doctor of Science (Technology) to be defended, with the permission of the Aalto University School of Chemical Engineering, at a public examination held via remote connection, on 08 January 2021 at 17:00.

Aalto University
School of Chemical Engineering
Department of Bioproducts and Biosystems
Biobased Colloids and Materials

Supervising professor
Professor Orlando Rojas, Aalto University, Finland

Thesis advisors
Doctor Blaise L. Tardy, Aalto University, Finland
Doctor Jukka Hassinen, Aalto University, Finland
Professor Orlando Rojas, Aalto University, Finland

Preliminary examiners
Associate Professor with Habilitation Miguel Gama, University of Minho, Portugal
Professor Guang Yang, Huazhong University of Science and Technology, China

Opponent
Professor Alexander Bismarck, University of Vienna, Austria

Aalto University publication series
DOCTORAL DISSERTATIONS 218/2020

ISBN 978-952-64-0202-4 (printed)
ISBN 978-952-64-0203-1 (pdf)
ISSN 1799-4934 (printed)
ISSN 1799-4942 (pdf)
http://urn.fi/URN:ISBN:978-952-64-0203-1

Images: Photography of cover image, Figure 7e and bacterial cellulose pellicle in Figure 2 by Valeria Azovskaya

Unigrafia Oy
Helsinki 2020

Finland

NORDIC SWAN ECOLABEL
Printed matter
4041-0619

Aalto University

Abstract

Aalto University, P.O. Box 11000, FI-00076 Aalto www.aalto.fi

Author
Janika Lehtonen

Name of the doctoral dissertation
Functional Materials from Nanocellulosic Networks and Uses in Water Purification

Publisher School of Chemical Engineering

Unit Department of Bioproducts and Biosystems

Series Aalto University publication series DOCTORAL DISSERTATIONS 218/2020

Field of research Bioproduct Technology

Manuscript submitted 4 September 2020 **Date of the defence** 8 January 2021

Permission for public defence granted (date) 18 November 2020 **Language** English

☐ **Monograph** ☒ **Article dissertation** ☐ **Essay dissertation**

Abstract

Due to their nano-scaled dimensions and mechano-chemical versatility, nanocelluloses have generated interest in the production of various types of bioproducts. However, the full potential of these materials and their applications, which are strongly coupled to their structural features, is yet to be realized. In this thesis, two types of nanocelluloses, cellulose nanofibrils (CNF) and bacterial nanocellulose (BNC), are introduced to achieve different types of porous networks and functional materials. The performance of CNF and CNF-based materials is investigated in applications related to water purification. Composites incorporating cationic CNF and silver nanoparticles are studied for use in drinking water disinfection. Phosphorylated CNF is implemented for the removal of uranium from water via batch adsorption. With BNC, the opportunities provided by biological fabrication of nanofibrous materials are considered in the synthesis of 2D membranes as well as intricate 3D structures. The impact of physico-chemical modifications of the fibrous networks in the BNC membranes are investigated to give insights on their potential use in pressure-driven filtration. To produce 3D structures from BNC, a simple method is developed utilizing hydrophobic particles for stabilization of air-water interfaces. Utilizing this method, capsules were produced and applied as sensors and enzymatic reactors in aqueous media. This thesis provides insights and novel pathways for the production and application of porous nanocellulose-based structures. They are expected to contribute to the development of future functional materials, for instance in the field of water purificaton.

Keywords Nanocellulose, Bacterial nanocellulose, Cellulose nanofibrils, Water purification

ISBN (printed) 978-952-64-0202-4 **ISBN (pdf)** 978-952-64-0203-1

ISSN (printed) 1799-4934 **ISSN (pdf)** 1799-4942

Location of publisher Helsinki **Location of printing** Helsinki **Year** 2020

Pages 156 **urn** http://urn.fi/URN:ISBN:978-952-64-0203-1

Tekijä
Janika Lehtonen

Väitöskirjan nimi
Funktionaalisia materiaaleja nanoselluloosaverkostoja hyödyntäen ja niiden käyttö vedenpuhdistuksessa

Julkaisija Kemian tekniikan korkeakoulu

Yksikkö Biotuotteiden ja biotekniikan laitos

Sarja Aalto University publication series DOCTORAL DISSERTATIONS 218/2020

Tutkimusala Biotuotetekniikka

Käsikirjoituksen pvm 04.09.2020 **Väitöspäivä** 08.01.2021

Väittelyluvan myöntämispäivä 18.11.2020 **Kieli** Englanti

☐ **Monografia** ☒ **Artikkeliväitöskirja** ☐ **Esseeväitöskirja**

Tiivistelmä

Selluloosananomateriaalien käyttö erilaisten biopohjaisten tuotteiden valmistamiseen on herättänyt kiinnostusta johtuen niiden nanomittakaavan koosta ja mekaanisesta ja kemiallisesta kestävyydestä. Näiden materiaalien ja niiden sovelluskohteiden täysi potentiaali on kuitenkin vielä saavuttamatta. Tässä väitöskirjassa on käytetty kahta eri typpistä selluloosananomateriaalia, selluloosananofibrillejä ja bakteeriselluloosaa, erityyppisten huokoisten verkostojen ja funktionaalisten materiaalien tuottamiseen. Selluloosananofibrilleistä koostuvista tai hyödyntävistä materiaaleista tutkittiin niiden suorituskykyä vedenpuhdistukseen liittyvissä sovelluskohteissa. Kationisia selluloosananofibrillejä ja hopeananopartikkeleita sisältävien komposiittien käyttöä tutkittiin juomaveden desinfektointiin. Fosforyloituja selluloosananofibrillejä käytettiin uraanin poistamiseen vedestä. Bakteeriselluloosan biologista valmistusprosessia hyödynnettiin kaksiulotteisten membraanien ja monimutkaisempien kolmiulotteisten rakenteiden muodostamiseen. Erilaisten fysikaalisten ja kemiallisten muokkausmenetelmien vaikutusta bakteeriselluloosamembraanien fibrilliverkostoon tutkittiin, jonka perusteella pystyttiin arvioimaan bakteeriselluloosamembraanien käytön potentiaalia paineen ajamana tapahtuvassa suodatuksessa. Kolmiulotteisten bakteeriselluloosa rakenteiden tuottamiseksi kehitettiin yksinkertainen menetelmä, jossa käytettiin hydrofobisia partikkeleita ilma-vesi rajapinnan stabiloimiseksi. Tällä menetelmällä tuotettiin kapseleita, joita tutkittiin sensoreina ja entsymaattisina reaktoreina vedessä. Tämä väitöskirja tarjoaa uusia havaintoja ja näkökulmia huokoisten nanoselluloosapohjaisten rakenteiden tuottamiseen ja käyttöön. Nämä voivat olla hyödyksi tulevaisuuden funktionaalisten materiaalien kehityksessä, esimerkiksi vedenpuhdistuksen alalla.

Avainsanat Nanoselluloosa, Bakteeriselluloosa, Selluloosa nanofibrillit, Vedenpuhdistus

ISBN (painettu) 978-952-64-0202-4 **ISBN (pdf)** 978-952-64-0203-1

ISSN (painettu) 1799-4934 **ISSN (pdf)** 1799-4942

Julkaisupaikka Helsinki **Painopaikka** Helsinki **Vuosi** 2020

Sivumäärä 156 **urn** http://urn.fi/URN:ISBN:978-952-64-0203-1

Acknowledgements

The work in this doctoral thesis was carried out in the Biobased Colloids and Materials (BiCMat) research group at Aalto University during 2016-2020. For funding of the research, the Center of Excellence in Molecular Engineering of Biosynthetic Hybrid Materials (HYBER) and the 3D-Manufacturing of Novel Biomaterials project funded by the Academy of Finland and the CelluClean project funded by Business Finland are acknowledged. Additionally, I would like to acknowledge the Foundation for Aalto University Science and Technology for the travel grant for my research visit to Australia.

As my time as a doctoral student is coming to an end, I want to express my gratitude to the people who have helped me in getting to this point. I feel very privileged to have had the possibility to work with so many amazing people throughout the course of my doctoral studies. The first person I would like to thank is my supervisor, Professor Orlando Rojas, first of all for giving me the chance to pursue a doctoral degree and for all the support he has provided for my research throughout these years. He has always been available for advice and discussion and his positivity and encouragement have helped me so much when I have had moments of doubt with my work. I also appreciate the effort he has put into creating and keeping up the great team spirit that we have in BiCMat. I joined the BiCMat group already in 2015 as a master's thesis student and it has been amazing to see how the group has grown since then, keeping the welcoming and supporting atmosphere throughout the years.

I also want to say a big thank you to my advisors, Blaise Tardy and Jukka Hassinen who have been incredibly supportive. I have learned a lot from both of them, including practical skills in the lab and how to compile results into the format of a scientific article and have enjoyed the many discussions, both scientific and non-scientific, we have had throughout these years. I also want to thank both Jukka and Blaise for their support in the writing process of this thesis and for the helpful feedback that improved the quality of this work. I would also like to acknowledge the pre-examiners, Professor Miguel Gama and Professor Guang Yang, for taking the time to examine this thesis and provide insightful feedback.

I want to express my gratitude to Ludovic Dumée and his group for all the support they provided during my research visit at Deakin University. I also want to thank my other co-authors (Anil, Luiz, Leena-Sisko, Heli, Roni, Riina, Anu, Xiao, Marco, Hannes, Jiaqi, Nikolaos, Professor Pradeep and Professor Ikkala), for their contribution to the articles included in this thesis. I want to specially thank Luiz Greca, it has been a pleasure to work with him in the lab and his creative ideas have brought interesting new directions to the bacterial cellulose work in our lab. I would also like to thank

Maryam and Mariko for the advice and guidance they provided, especially in the beginning of my doctoral studies. The technical staff at Bio2 has always been very helpful and I want to give a special thank you to Rita, Marja, Tuyen, Leena, Timo, Terho and Risu.

Being a doctoral student can get stressful at times and therefore being part of a research group that you can rely on both for support in your work and also to get your mind off of research for a while has been something that I have truly valued during these years. I want to thank all past and present members of BiCMat that I have had the chance to interact with. A special thank you to Blaise, Rubina, Joice, Eva, Gisela, Tai, Bruno, Wenchao, Mariko, Maryam, Jiaqi, Luiz, Marco, Leena-Sisko, Meri, Tero, Anu, Caio, Gabi, Carlos, Antonio, Katariina, Roozbeh, Bin, Urs, Emily, Nikorn, Johanna, Siqi, Long, Yang, Gonghua, Monir, Konrad and Guillermo for all the great moments spent inside and outside of the department including Aalto Inn gatherings, playing frisbee and other sports, various trips and many other events. A big thank you to Ling for your friendship and being my wonderful officemate since our master's thesis times, the PhD journey would not have been the same without you. I want to also thank others in the department for all the fun conversations in the coffee rooms, labs and corridors of the Puu 1 building. Especially these times of social distancing we are currently living in have made me realize how much energy the work community at the department has given me throughout these years. I also want to thank the friends I made during my visit to Australia, Rania, Priyanka and Yun, for the lunch break discussions at the IFM cafe and many great memories exploring Australia together.

I am also very grateful to my friends outside of research life, a special mention to the Böröt group. And finally, a big thank you to my mom, dad and my sister, for your support and for always being there for me. I have faced plenty of challenges on the road to finishing this doctoral thesis, but these years have also included many rewarding moments and countless memories I will never forget.

Espoo, November 2020
Janika Lehtonen

List of Publications

This doctoral dissertation consists of a summary and of the following publications, which are referred to in the text by their Roman numerals.

Paper I. Lehtonen, Janika; Hassinen, Jukka; Kumar, Avula Anil; Mäenpää, Roni; Johansson Leena-Sisko; Pahimanolis, Nikolaos; Pradeep, Thalappil; Ikkala, Olli; Rojas, Orlando J. Phosphorylated cellulose nanofibers exhibit exceptional capacity for uranium capture. Accepted for publication in the journal *Cellulose* in 2020. DOI 10.1007/s10570-020-02971-8

Paper II. Lehtonen, Janika; Hassinen, Jukka; Honkanen, Riina; Kumar, Avula Anil; Viskari, Heli; Kettunen, Anu; Pahimanolis, Nikolaos; Pradeep, Thalappil; Rojas, Orlando J.; Ikkala, Olli. 2019. Effects of chloride concentration on the water disinfection performance of silver containing nanocellulose-based composites. *Scientific Reports*, 9, 19505. DOI 10.1038/s41598-019-56009-6

Paper III. Lehtonen, Janika; Chen, Xiao; Beaumont, Marco; Hassinen, Jukka; Orelma, Hannes; Dumée, Ludovic F.; Tardy, Blaise L.; Rojas, Orlando J. 2021. Impact of incubation conditions and post-treatment on the filtration properties of bacterial nanocellulose membranes. *Carbohydrate Polymers*, 251, 117073. DOI 10.1016/j.carbpol.2020.117073

Paper IV. Greca, Luiz G.; **Lehtonen, Janika**; Tardy, Blaise L.; Guo, Jiaqi; Rojas, Orlando J. 2018. Biofabrication of multifunctional nanocellulosic 3D structures: a facile and customizable route. *Materials Horizons*, 5(3), 408-415. DOI 10.1039/C7MH01139C

Author's Contribution

Paper I: Phosphorylated cellulose nanofibers exhibit exceptional capacity for uranium capture

JL wrote the initial manuscript draft with the assistance of JH and under the supervision of OJR and performed adsorption studies and SEM imaging. RM and JH contributed to planning of the adsorption experiments. TEM imaging was done by JH and ICP-MS measurements were conducted by AAK. LSJ was responsible for the XPS analysis. The phosphorylated and TEMPO oxidized nanofibrils were provided by NP on behalf of Betulium Ltd. The manuscript was reviewed by JH, AKK, RM, LSJ, NP, TP, OI and OJR.

Paper II: Effects of chloride concentration on the water disinfection performance of silver containing nanocellulose-based composites

JL wrote the initial manuscript draft with the assistance of JH under the supervision of OJR and performed antibacterial tests. RH, HV, and AK participated in the design of antibacterial tests. JL and JH prepared the composites and performed experiments related to composite characterization. Water samples from India were collected by RH and AAK. AAK conducted the ICP-MS measurements. Cationic cellulose nanofibrils were provided by NP on behalf of Betulium Ltd. The manuscript was reviewed by RH, AAK, HV, AK, NP, TP, OJR and OI.

Paper III: Impact of incubation conditions and post-treatment on the filtration properties of bacterial nanocellulose membranes

JL wrote the manuscript together with BLT and conducted filtration experiments, SEM imaging and capillary flow porometry experiments. The experimental work was carried out under the supervision of LFD, BLT, and OJR. XC conducted profilometry experiments and MB conducted testing under compressive load. BLT, JH, HO, LFD and OJR participated in planning of experimental work. The manuscript was reviewed by all co-authors.

Paper IV: Biofabrication of multifunctional nanocellulosic 3D structures: a facile and customizable route

JL participated in writing the manuscript together with LGG and BLT. The work was carried out under the supervision of BLT and OJR. JL prepared the bacteria cultures used, conducted SEM imaging and the gravimetric and permeability study of the capsules. LGG produced and characterized the structures with complex morphologies, conducted the mechanical testing and bio-welding study and was the main responsible for the graphic design and photography. BLT conducted cargo encapsulation and kinetic study of encapsulated enzyme. JG produced the gold nanoparticles. The manuscript was reviewed by all authors.

List of Abbreviations and Symbols

AgNP	Silver nanoparticle
AuNP	Gold nanoparticle
BNC	Bacterial nanocellulose
BET	Brunnauer-Emmett-Teller
BSA	Bovine serum albumin
cCNF	Cationic cellulose nanofibrils
CFU	Colony forming unit
CNC	Cellulose nanocrystals
CNF	Cellulose nanofibrils
DBNC	Dried bacterial nanocellulose
EDX	Energy dispersive X-ray
FT-IR	Fourier transform infrared
LB	Luria Bertani
MOF-HRP	Metal organic framework encapsulated horseradish peroxidase
NDBNC	Never-dried bacterial nanocellulose
PHO-CNF	Phosphorylated cellulose nanofibrils
POE	Poly(oxyethylene)
PTFE	Polytetrafluoroethylene
PWF	Pure water flux
SEM	Scanning electron microscopy
TEM	Transmission electron microscopy
TO-BNC	TEMPO oxidized bacterial nanocellulose
TO-CNF	TEMPO oxidized cellulose nanofibrils
UO_2^{2+}	Uranyl ion
UV-Vis	Ultraviolet-visible
XPS	X-ray photoelectron spectroscopy

Contents

Acknowledgements
List of Publications
Author's Contribution
List of Abbreviations and Symbols
1. Introduction 1
2. Background 4
2.1 Nanocelluloses 4
2.1.1 Cellulose Nanofibrils 5
2.1.2 Bacterial Nanocellulose 5
2.1.3 Comparison of Nanocellulose Types 6
2.2 Porous Nanocellulosic Structures 7
2.2.1 Gelation of Nanocelluloses 7
2.2.2 3D Structures of Bacterial Nanocellulose 8
2.2.3 Aerogels, Nanopapers and Composites 9
2.3 Utilization of Nanocelluloses for Water Treatment 11
2.3.1 Sorption of Heavy Metals and Other Contaminants 11
2.3.2 Pressure-driven Membrane Separation 12
2.3.3 Water Disinfection 13
3. Materials and Methods 15
3.1 Cellulose Nanofibrils and Preparation of Composites 15
3.2 Production of Bacterial Nanocellulose Structures 15
3.3 Characterization Methods Used 16
3.4 Adsorption of Uranium 17
3.5 Characterization of Fibrils After Adsorption of Uranium 18
3.6 Antibacterial Tests with Composites 18
3.7 Filtration Studies with Bacterial Nanocellulose 19
3.8 Functionalities of 3D structures 20
4. Results and Discussion 22
4.1 Studies Utilizing Cellulose Nanofibrils 22

4.1.1 Characterization of Cellulose Nanofibrils 22
4.1.2 Uranium Adsorption 23
4.1.3 Antibacterial Activity of the Composites 25
4.2 Studies with Bacterial Nanocellulose 28
4.2.1 Pressure-driven Filtration with Bacterial Nanocellulose 28
4.2.2 Biofabrication of Nanocellulosic 3D Structures 30
5. Concluding Remarks and Prospects 34
References 35

1. Introduction

To meet the concerns on the environmental impact of non-renewable materials, interest in the opportunities offered by the use of sustainable biobased materials is growing. Cellulose, as an abundant and renewable resource, is well-known for its traditional use in paper-based products and textiles. However, the potential of engineering cellulose for production of high-performance functional materials, beyond such traditional uses, has recently received significant interest and remains a highly relevant research topic. In addition to the use of macroscale cellulose fibers, such as conventional pulp fibers, research interest on the use of nanoscale cellulose materials has been growing. This is due to the unique properties exhibited by nanocelluloses, resulting from their high specific surface area, aspect ratio and easy functionalization due to their abundant surface hydroxyl groups (Moon *et al.*, 2011; Klemm *et al.*, 2011; Habibi, 2014). Owing to their properties, nanocelluloses can be structured into various types of architectures, which open new potential applications and functionalities. Nanocelluloses have found application for instance in the packaging sector (Klemm *et al.*, 2018; Kontturi *et al.*, 2018; De France *et al.*, 2020), biomedical materials (Klemm *et al.*, 2018; Kontturi *et al.*, 2018; De France *et al.*, 2020), reinforcement of composites (Klemm *et al.*, 2018; De France *et al.*, 2020), energy storage (Chen *et al.*, 2018; Klemm *et al.*, 2018; De France *et al.*, 2020) and as viscosity modifiers and interfacial stabilizers (Klemm *et al.*, 2018; Kontturi *et al.*, 2018; De France *et al.*, 2020).

In addition to the need for reducing the environmental impact of materials, challenges related to water are a major global concern (Mekonnen and Hoekstra, 2016). As human population grows, the demand of agricultural and industrial resources also increases. Accordingly, new technologies and innovations are needed to ensure availability of safe drinking water. Energy-efficient solutions that provide microbially safe and contaminant-free water at low-cost are urgently needed (Sankar *et al.*, 2013; Lee, Elam and Darling, 2016). The possibilities of using advanced materials and nanotechnology have been brought up as promising tools for developing future water treatment materials (Nagar and Pradeep, 2020). Cellulose nanomaterials and their structures can potentially provide new types of solutions for materials needed for water treatment.

This thesis introduces the production and characterization of different types of porous materials and networks consisting of nanocelluloses or containing nanocelluloses. Their nanoscale dimensions and unique properties such as high aspect ratio and facile functionalization were utilized to produce functional materials. The properties of the produced structures, including their porosity, hydrophilicity and their

interaction with water, were explored for water treatment, ranging from freshwater purification to pressure-driven membrane separation. The focus was on producing materials that could potentially be produced at low-cost without the use of energy-intensive drying methods (**Papers I, II, III, IV**). Two types of cellulose nanomaterials, namely cellulose nanofibrils (CNF) and bacterial nanocellulose (BNC), were utilized in the work reported in this thesis. The production processes to obtain these materials differ significantly. CNF is produced by a top-down process typically from plant-based raw-materials. BNC is obtained by a bottom-up biofabrication process using sugars as building blocks. Many of the material properties of BNC and CNF are connected to their production method. Therefore, the production method also has a key role when considering the properties of different types of BNC or CNF structures. In **Papers I** and **II**, commercial functionalized CNF was used to demonstrate cost-effective materials for water purification. In **Papers III** and **IV**, the goal was to explore the potential of BNC by using its native structure in the wet state, either as membranes (**Paper III**) or in more complex 3D structures (**Paper IV**). The outline of this thesis is summarized in Figure 1, presenting the different connections considered. The research questions investigated in each paper, related to the structure produced and its potential application, are specified below. A short background on the motivation of each study is also provided.

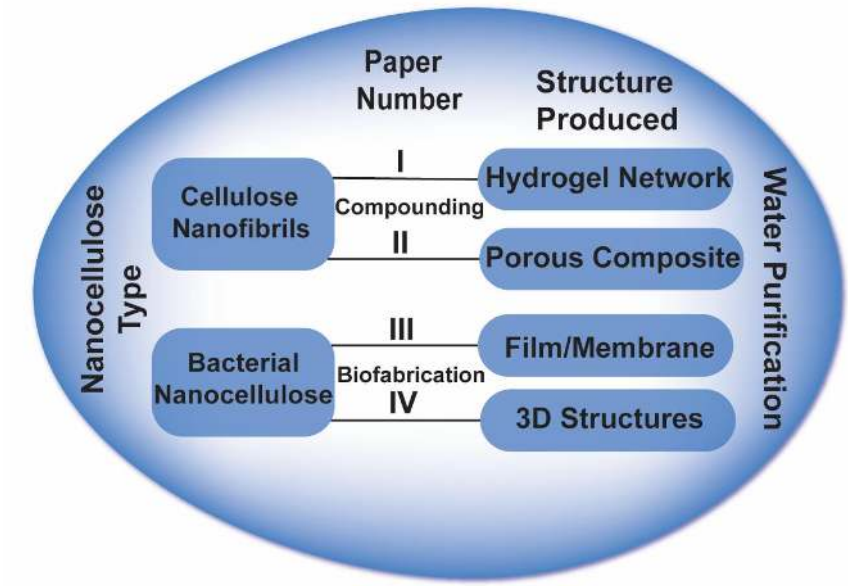

Figure 1. General outline of this thesis.

Paper I: Can CNF be functionalized to allow removal of uranium in water? If this happens, what is the mechanism of removal?

Uranium is a toxic, radioactive heavy metal found in natural waters due to leaching from mineral deposits or as a result of industrial activities such as mining. Solutions for removing uranium from water are needed due to possible harmful effects of uranium on human health and the environment (Xie *et al.*, 2019). Adsorption is one of

the methods that has been proposed for uranium removal from water. In **Paper I** the use of phosphorylated cellulose nanofibrils (PHO-CNF) for removal of uranium from water by adsorption is studied.

Paper II: Can point-of-use water disinfection materials utilizing CNF be produced? How would these materials perform in natural freshwaters?
The availability of microbially safe drinking water is a concern in many rural areas and developing countries. Materials that can be applied in point-of-use disinfection have been proposed as a solution. In **Paper II** nanocellulose is used to produce a composite material for point-of-use water disinfection and the effect of different chloride concentrations typically present in freshwaters on the antibacterial activity of the material is investigated.

Paper III: How does applied pressure affect the BNC network structure and how will different modifications of BNC membranes influence their filtration properties? Are BNC membranes applicable for the separation of macromolecules by pressure-driven filtration?
BNC has proven to be appealing for material development due to its unique properties. The potential of BNC as a separation material has been studied, but factors affecting the use of BNC as a membrane for pressure-driven separation have not been comprehensively studied. In **Paper III**, the properties of BNC relevant for pressure-driven membrane separation are evaluated, including pure water fluxes (PWF) and rejections of macromolecules. These properties provide indirect insights on the pore sizes and porosity of BNC when in aqueous conditions and subjected to pressure, which are typically not attainable with traditional pore characterization methods.

Paper IV: Can customizable nanocellulosic 3D structures be produced by a simple method utilizing biofabrication with living micro-organisms? What type of functionalities could be provided by cargo encapsulation into these structures?
Several limitations have hindered the development of advanced 3D structures consisting of BNC. Better control of 3D structured BNC films across several length scales could allow the production of advanced nanocellulosic materials with a wider range of applications. In **Paper IV**, a novel method for production of nanocellulosic 3D structures using bacteria is presented and the potential for the use of these materials by including encapsulated cargo is explored.

2. Background

2.1 Nanocelluloses

The term nanocellulose refers to the cellulosic materials having at least one dimension in the nanoscale (Klemm *et al.*, 2018). Generally, nanocelluloses are divided into three categories: cellulose nanofibrils (CNF), bacterial nanocellulose (BNC) and cellulose nanocrystals (CNC). The three different types of nanocelluloses are pictured in Figure 2. CNF is also referred to as nanofibrillated cellulose and in some cases also as microfibrillated cellulose. BNC is nanocellulose produced by bacteria and is also referred to as bacterial cellulose or microbial cellulose. CNC, also termed as cellulose nanowhiskers, are rod-like particles (50-500 nm in length and 3-5 nm in width) produced by extracting the crystalline regions of the cellulose structure by acid hydrolysis (Dong, Revol and Gray, 1998; Moon *et al.*, 2011). The nanocellulose types utilized in this thesis include BNC and CNF, which are introduced and compared in the next sections.

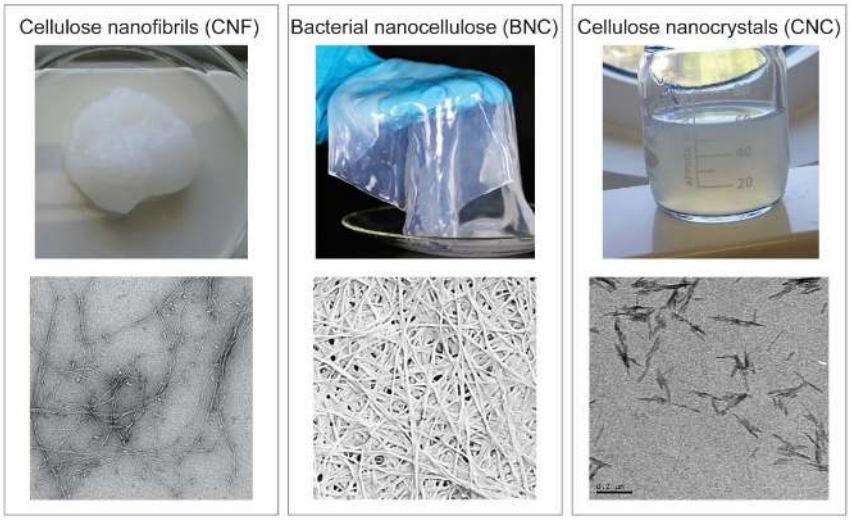

Figure 2. Structures of the different types of nanocelluloses. From left to right, the images on the top show a cellulose nanofibril (CNF) hydrogel, a bacterial nanocellulose (BNC) pellicle and a cellulose nanocrystal (CNC) suspension. The images on the bottom indicate the entangled fibril structure of CNF, 3D fibril network structure of BNC and the rod shape of CNC.

2.1.1 Cellulose Nanofibrils

CNF can be produced from cellulose extracted from wood, various plants, algae or tunicates (Moon *et al.*, 2011). The manufacture of CNF by high pressure homogenization was pioneered in the US in the early 1980s by Herrick *et al.* and Turbak *et al.* (Herrick *et al.*, 1983; Turbak *et al.*, 1983). The typical manufacturing process includes mechanical disintegration with or without pretreatment. High pressure homogenization (Stelte and Sanadi, 2009), microfluidization (Rajala *et al.*, 2016) and grinding (Iwamoto, Abe and Yano, 2008) are examples of mechanical treatments that have been used for CNF production. Pretreatment methods, including enzyme treatment (Henriksson *et al.*, 2007; Pääkkö *et al.*, 2007) and chemical treatment such as TEMPO oxidation (Saito *et al.*, 2007), carboxymethylation (Wågberg *et al.*, 2008), phosphorylation (Ghanadpour *et al.*, 2015), sulfonation (Liimatainen *et al.*, 2013) and cationization (Olszewska *et al.*, 2011), have been used to reduce the energy consumed in the production process. Additionally, the chemical pretreatment methods introduce functional groups on the surface of the fibrils. This results in surface charges on the fibrils, leading to increased interfibrillar repulsion.

The size of CNF varies depending on the preparation process, with typical widths varying from 5 nm to 20 nm and lengths of up to several micrometers. Using pretreatment in the preparation process typically results in lower widths, for example widths of 3-4 nm have been reported after TEMPO oxidation (Saito *et al.*, 2007). CNF contains both crystalline and amorphous regions. As such, the crystallinity of CNF varies depending on the source and preparation method (Sacui *et al.*, 2014). Excellent mechanical properties for CNF have been reported with strengths of individual wood CNF being in the range of 1.6 to 3 GPa and for tunicate CNF in the range of 3 to 6 GPa (Saito *et al.*, 2013).

2.1.2 Bacterial Nanocellulose

The discovery of BNC is assigned to A.J. Brown. He reported the cellulose producing ability of the *Acetobacter* genus (which has been reclassified as *Komagataeibacter*) (Brown, 1886). Since then, several other families of bacteria have been reported to produce cellulose, including *Azotobacter*, *Sarcina* and *Pseudomonas*. However, *Acetobacter* remains as the most studied bacteria for BNC production (Ross, Mayer and Benziman, 1991). BNC has the same chemical structure as cellulose from plant origin, consisting of glucose units linked by 1,4 glucosidic bonds. Research interest on BNC has been increasing since the 1980s when the excellent mechanical properties of BNC were reported (Yamanaka *et al.*, 1989).

In the BNC production process, bacteria use sugars to produce cellulose that is then secreted by the bacteria as nanoscale fibrils, with widths in the 20-100 nm range (Klemm *et al.*, 2011). Bacteria from the *Komagataeibacter* genus are aerobic, leading to cellulose production at the air-medium interface, where the bacteria have access to oxygen. The cultivation conditions, the organism used, the composition of the culture medium and carbon source used influence the properties of the BNC produced (Ul-islam, Khan and Park, 2012). The reason behind the production of cellulose by bacteria is still under debate but it has been proposed to be a protection mechanism against UV light or a way for the bacteria to sustain their position at the surface of the culture

medium (Iguchi, Yamanaka and Budhiono, 2000). After the incubation process, bacteria can easily be removed from BNC by immersion into dilute alkaline solution (Iguchi, Yamanaka and Budhiono, 2000). Compared to plant celluloses, BNC has higher purity, degree of polymerization and crystallinity (Klemm *et al.*, 2005). The high water retention value of BNC, which consists of approximately 99% water in its never dried state, gives it a hydrogel-like character (Gelin *et al.*, 2007). The unique properties of BNC in addition to its good compatibility with living tissues (Fu *et al.*, 2013) and lack of genotoxicity suggested by in vitro assays (Moreira *et al.*, 2009) have resulted in applications of BNC in the biomedical field.

2.1.3 Comparison of Nanocellulose Types

The structural differences of BNC, CNF and CNC are key when comparing the application potential of these materials. When considering BNC, the unique 3D network structure presents several advantages as discussed in **Papers III** and **IV**, whereas the high surface area of CNF provided by the individual or bundled nanoscale fibrils is a very useful property for several applications, including those related to the adsorption of heavy metals, as studied in **Paper I** or as a reinforcing component in composites, as demonstrated in **Paper II**. CNC as individual or bundled nanocrystals also provide high surface area and can be useful when applied similarly as mentioned for CNF. In this work, BNC and CNF were chosen in order to study the use of fibrous cellulose nanomaterials in two different forms.

The key challenge when using CNF for water-related applications is how to produce structures that are stable in water and have adequate mechanical strength when exposed to water, especially when considering functionalized fibrils, which typically exhibit strong repulsive forces due to electrostatic charge. Potential ways to solve these issues could be physical or chemical crosslinking of the fibrils or producing composite structures, as demonstrated in **Paper II**. In the case of BNC, the native 3D network structure formed during the incubation phase of the material provides good stability in water. The structural differences of the materials also influence the functionalizability of the materials. Chemical modification on the surface of the BNC fibril network is rather easy to achieve; however, functionalizing the whole network is challenging. With CNF, a high degree of surface functionalization can be achieved due to the high surface area provided by the individual fibrils. In terms of modifying the network, the biological production method of BNC presents interesting alternatives such as varying culture medium composition. As a result, when aiming to control the properties of structures produced from BNC, a critical factor is to understand to what extent the biological production process can be controlled. In the case of CNF, control on crosslinking or other procedures used for the formation of the structures are crucial. It should be noted that the 3D network structure of BNC can also be disintegrated by mechanical treatment to achieve materials with similar properties than those of CNF. However, in this thesis BNC was used in its native structure, as a 3D network. In this way the full benefit of the biological production process is utilized.

When it comes to raw materials, the cellulose fibers used for producing CNF or CNC are obtained from different wood or plant sources. In contrast, for BNC, sugars can be obtained from different types of industrial residues. Alternative feedstocks such as recycled paper and paper industry sludge for CNF and CNC production have been

considered (Carpenter, De Lannoy and Wiesner, 2015). However, further improvements in the energy and chemical efficiency and cost-effectiveness are important to consider for future developments in CNF production. For BNC, decreasing the cost of the production process is a key challenge (da Gama and Dourado, 2018). Even though as a raw material cellulose is eco-friendly, the effect of the modification and other processing steps used to produce nanocellulose materials need further consideration in terms of sustainability and cost (Hokkanen, Bhatnagar and Sillanpää, 2016).

2.2 Porous Nanocellulosic Structures

Due to their stiffness and strength, cellulose nanomaterials are useful building blocks in the formation of various types of mechanically robust and functional structures (Moon *et al.*, 2011; Saito *et al.*, 2011; Kontturi *et al.*, 2018; De France *et al.*, 2020). When forming assemblies of CNC or CNF, the dispersion, entanglement, aggregation and alignment of the fibrils or crystals often needs consideration when attempting the control of morphology. In the case of BNC, as stated earlier, the biological production process allows for manipulation of the material properties by controlling the incubation conditions. This section introduces different types of porous nanocellulose structures and how they are formed. Both never dried and dry materials with different types of network topologies are covered.

2.2.1 Gelation of Nanocelluloses

Hydrogels are classified as polymer networks that are swollen by a considerable amount of trapped water. Hydrogels are formed by physical bonding through supramolecular bonds such as ionic or hydrogen bonds or through covalent bonds. When the concentration of CNF is above a certain level (0.5-1%), a hydrogel is formed (Kontturi *et al.*, 2018). However, gel-like behavior already at a concentration of 0.125% has been reported for CNF produced by enzymatic hydrolysis followed by mechanical treatment (Pääkkö *et al.*, 2007). For CNCs much higher concentration is needed for gelation (Kontturi *et al.*, 2018; De France *et al.*, 2020) and a gelation threshold of 6% has been reported (Liu *et al.*, 2019). The colloidal stability of nanocellulose gels is affected by pH and electrolyte concentration (Mendoza *et al.*, 2018). For native CNF, interfibrillar hydrogen bonds challenge fibril dispersion in aqueous solutions. In contrast, surface modification to introduce charges on the fibrils prevents aggregation and enhances the water dispersibility.

Hydrogels from charged fibrils have been prepared by alkaline treatment (Abe and Yano, 2011), lowering pH (Saito *et al.*, 2011) or using additives including salts, surfactants and alcohols (Schmitt *et al.*, 2018). The addition of electrolytes has been found to screen the repulsive forces between the charged fibrils, thus, favouring gelation (Fukuzumi *et al.*, 2014). It should be noted that the change from repulsion between fibrils to aggregation is dependent on the concentration of the electrolytes (Schmitt *et al.*, 2018). The addition of several different metal ions, including Ag^{+} (Dong *et al.*, 2013a), Zn^{2+}, Cu^{2+}, Al^{3+}, Fe^{3+} (Dong *et al.*, 2013b) and UO_2^{2+} (Ma, Hsiao and Chu, 2012) has been found to trigger the gelation of TEMPO oxidized CNF (TO-CNF). This could be attributed to the association of the functional groups on the CNF with the metal ions. It should be noted that TO-CNF can also form stable gels without the

presence of cations (Mendoza *et al.*, 2018). Recent developments in the extrusion of CNF hydrogels using 3D printing for producing various types of materials have been reported (Håkansson *et al.*, 2016; Sultan *et al.*, 2017; Ajdary *et al.*, 2019). BNC can also be considered as a hydrogel in its never dried state, since it generally contains around 99% water. Around 10 % of the water in the BNC network has been found to behave as free bulk water with the rest of the water being bound to the cellulose network (Gelin *et al.*, 2007). Porous materials can be produced by drying nanocellulose hydrogels using various approaches. These are introduced in section 2.2.3.

2.2.2 3D Structures of Bacterial Nanocellulose

New methods for utilization of systems containing living micro-organisms to produce 3D materials, also referred to as 3D biofabrication, have been developed in recent years (Nguyen *et al.*, 2018). The use of living micro-organisms also opens new possibilities for the formation of advanced nanocellulosic architectures. When BNC is grown statically, a film of cellulose nanofibers, typically referred to as a pellicle, forms at the surface of the culture medium. In agitated cultures, BNC with spherical shape has been produced (Hu and Catchmark, 2010; Zhu *et al.*, 2011). The formation of BNC at the air-water interface enables the formation of robust structures from 2D films with controlled microtopography to different types of 3D morphologies. The various possibilities to mold BNC during its production process without causing significant changes in its physical properties, are a great advantage of the material (Czaja *et al.*, 2007). 3D structures of BNC have been produced using several different approaches, including the use of oxygen-permeable molds, 3D printing and foam templating. All these techniques utilize the concept of controlling the air-liquid interface, where the BNC production occurs. The use of oxygen permeable molds is the most frequently reported method in literature and has been used for the production of tubes for use as artificial blood vessels (Klemm *et al.*, 2001; Andrade *et al.*, 2013) or in protein separation (Orelma *et al.*, 2014), ear cartilage (Nimeskern *et al.*, 2013) and for structuring the BNC surface (Bottan *et al.*, 2015; Geisel *et al.*, 2016). Molds are typically made from silicone. Bottan *et al.* used a surface structured PDMS mold that led to the alignment of BNC fibers. This method could improve the cell interaction of BNC and have possible use in the field of wound healing and tissue regeneration. Geisel *et al.* used a similar approach for structuring BNC with silicone and PDMS molds for the guided growth of neural stem cells, with patterned structures of 5 μm in width and 20 μm in height produced (Geisel *et al.*, 2016).

In addition to the approach of using oxygen permeable molds, alternative methods have been investigated for the formation of 3D structures from BNC. The concept of using 3D printing was introduced by Schaffner *et al.* (Schaffner *et al.*, 2017). In their method, bacteria and culture medium components were incorporated into the ink used for 3D printing. The critical factors for the BNC formation were oxygen availability and the viscosity of the ink. Compared to the mold-based method, a further freedom of shape is provided by the 3D printing technique; however, the viscosity of the ink can limit the growth conditions of the bacteria. Shin *et al.* used solid matrix-assisted 3D printing for producing tubular BNC structures (Shin *et al.*, 2019). Rühs *et al.* introduced the foam forming approach where a suspension of bacteria and foam forming agent is used to produce microporous structures of BNC for tissue

engineering. The formation of cellulose had a foam stabilizing effect (Rühs *et al.*, 2018). The main limitations of the techniques presented here are related either to the mold material and slower growth rate due to lower oxygen availability (Putra *et al.*, 2008), the control over the morphology of the produced objects or need for addition of extra components to the culture medium in order to stabilize the structure. Figure 3 summarizes some of the most typical approaches reported for structuring BNC.

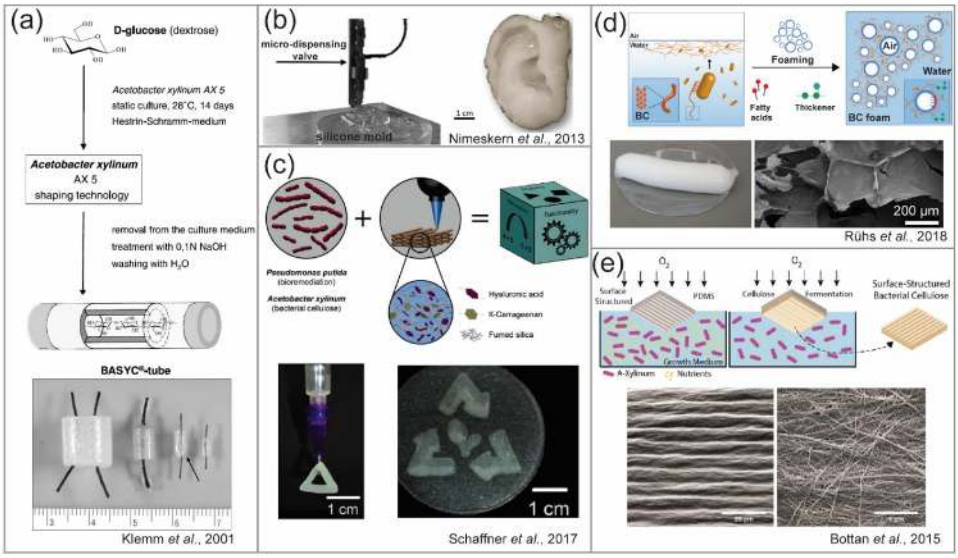

Figure 3. Different approaches for structuring bacterial nanocellulose (BNC). (a) Production of BNC tubes using oxygen permeable molds for application as artificial blood vessels. Adapted from Klemm *et al.*, 2001 with permission from Elsevier. (b) Production of BNC for ear cartilage replacement using a silicone mold. Adapted from Nimeskern *et al.*, 2013 with permission from Elsevier. (c) Using an ink containing BNC producing bacteria for 3D printing and incubation of the printed structures to produce BNC. Adapted from Schaffner *et al.*, 2017 with permission under the Creative Commons Attribution NonCommercial License 4.0 (CC BY-NC). (d) Foam templating approach for production of BNC structures. Adapted from Rühs *et al.*, 2018 with permission under the Creative Commons Attribution NonCommercial License 4.0 (CC BY-NC). (e) Surface structuring of BNC using PDMS molds. Adapted from Bottan *et al.*, 2015 with permission from the American Chemical Society.

2.2.3 Aerogels, Nanopapers and Composites

Porous materials produced by drying of nanocellulose gels include aerogels, foams and nanopapers. Aerogels are materials with high porosity, low density and high strength-to-weight ratio, with up to 95 % of their volume being air (Hüsing and Schubert, 1998). Aerogels are formed by replacing the liquid in a hydrogel or dispersion with gas using drying methods that do not cause shrinkage (Sehaqui *et al.*, 2010). Aerogels from cellulose nanomaterials are typically formed from hydrogels or dispersions by freeze drying or critical point drying to prevent the collapse of the fibril

network (Pääkkö *et al.*, 2008; Ferreira *et al.*, 2020). Aerogels have been made using native CNF (Pääkkö *et al.*, 2008), carboxylated CNF (Saito *et al.*, 2011), CNCs (Heath and Thielemans, 2010) and BNC (Olsson *et al.*, 2010). The morphology, surface properties and concentration of CNF have been shown to influence the structure of the aerogels (Chen *et al.*, 2014). A strong, flexible aerogel network without the need for crosslinking can be obtained using unmodified CNF (Pääkkö *et al.*, 2008). The high adsorption capacity, low thermal conductivity, low dielectric constant and good mechanical properties make CNF and CNC aerogels promising for application in thermal insulation (Gupta *et al.*, 2018), energy storage (Zu *et al.*, 2016) and as absorbents (Korhonen *et al.*, 2011). However, the commonly used drying processes for aerogel preparation are energy intensive and time consuming (Kobayashi, Saito and Isogai, 2014). Another challenge for several applications is that nanocellulose aerogels can easily disintegrate in water unless cross-linking or physical gelation with different treatments is applied (Jiang and Hsieh, 2014a). Cross-linkers such as methylene diphenyl diisocyanate (Jiang and Hsieh, 2017) and polyamide-epichlorohydrin resin (Zhang *et al.*, 2012) have been used to produce aerogels that are stable in water.

CNF dispersed in aqueous solution can also be formed into nanopapers. Nanopapers have been defined as networks of entangled nanofibrils in random in-plane orientation (Henriksson *et al.*, 2008). Nanopapers are typically produced by filtering CNF dispersed in water to produce a hydrogel film, which is then dried by applying pressure and temperature on the filtered film. Compared to the previously introduced aerogels, nanopapers have a much denser structure resulting from nanofiber aggregation during the drying process. However, the porosity can be increased by using similar drying methods as for aerogels (Henriksson *et al.*, 2008; Sehaqui *et al.*, 2011) or by treatment with organic solvents including acetone (Henriksson *et al.*, 2008; Karim *et al.*, 2016). CNF nanopapers typically have significantly better mechanical properties compared to traditional paper (Kontturi *et al.*, 2018).

The biodegradability, excellent mechanical properties and low density of nanocellulosic materials make them promising for use as reinforcement in composites. When using nanofibrils for reinforcement, the fibril size, fibril/matrix adhesion, fibril content in the composite and fiber orientation all affect the properties of the fibril-reinforced composite (Dufresne and Paillet, 2002). Composites are often divided into materials with a hydrophilic matrix and materials with a hydrophobic matrix. The natural hydrophilicity of cellulose nanomaterials makes them ideal for combining with hydrophilic polymers but chemical modifications can be used to facilitate incorporation with hydrophobic polymers (Siró and Plackett, 2010). In addition to combinations with polymers such as poly(lactic acid) and poly(vinyl alcohol), nanocelluloses have been compounded with various other materials, including clays (Liu *et al.*, 2011; Wu *et al.*, 2012; Hokkanen *et al.*, 2018) and graphene oxide (Jiang *et al.*, 2019; Xing *et al.*, 2019). Besides improving mechanical properties, nanocelluloses can enhance thermal and barrier properties of the produced composites. Even small concentrations of cellulose nanomaterials have been found to form an efficient network for increasing the mechanical performance of composites (Favier *et al.*, 1995).

2.3 Utilization of Nanocelluloses for Water Treatment

Nanotechnology has emerged as a promising field for developments in materials used for water treatment. Nanocelluloses have been applied as water treatment materials in various material architectures including aerogels and hydrogels for adsorption, nanopapers for filtration, and solid materials for controlled release of active particles (Sharma *et al.*, 2020). Common processes used in water treatment include membrane processes, liquid extraction, flocculation, coagulation, adsorption and electrodialysis. Among these adsorption and membrane separation are the most common types of processes where the use of nanocelluloses has been studied. The following sections introduce these processes. Figure 4 presents a summary of the main structures, separation principles and applications involved in the use of nanocelluloses for water treatment.

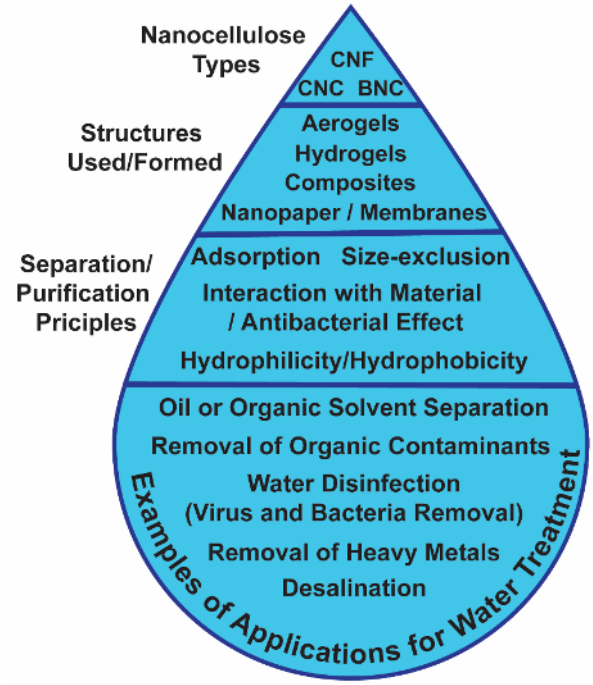

Figure 4. Application of nanocelluloses for water treatment.

2.3.1 Sorption of Heavy Metals and Other Contaminants

Adsorption has several advantages over other commonly used water treatment methods, including simplicity, low cost and energy efficiency. The high aspect ratio, surface area and functionalizability of nanocelluloses has made them a promising option for the removal of contaminants by adsorption and a considerable alternative to traditional adsorbents such as activated carbon. A vast amount of studies on the use of functionalized nanocelluloses for heavy metal removal have been conducted. Typically the adsorption capacity of nanocellulose materials for heavy metals is improved by different chemical modifications, such as carboxylation (Yu *et al.*, 2013),

phosphorylation (Oshima *et al.*, 2008; Liu *et al.*, 2015), succinylation (Hokkanen, Repo and Sillanpää, 2013), sulfonation (Suopajärvi *et al.*, 2015), TEMPO oxidation (Ma, Hsiao and Chu, 2012; Sehaqui *et al.*, 2014) and amination (Shen *et al.*, 2009; Hokkanen *et al.*, 2014; Singh, Sinha and Srivastava, 2015). In some cases grafting of polymers with functional groups onto cellulose nanomaterials has also been used (Zhang *et al.*, 2014a). The nature and density of the functional groups are important factors in determining the adsorption capacity of the materials (Abouzeid *et al.*, 2019). When conducting studies with these materials it should also be considered that heavy metals can exist as different species in water depending on the aqueous environment. To ensure efficient adsorption, the identification of these species is critical (Voisin *et al.*, 2017).

In addition to heavy metal removal, functionalized cellulose nanomaterials have been demonstrated for adsorption of dyes (Batmaz *et al.*, 2014; Chan *et al.*, 2015), negatively charged contaminants (Sehaqui *et al.*, 2016a) and pharmaceutical molecules (Rathod, Haldar and Basha, 2015). Additionally, nanocellulose aerogels have been studied for absorption of oil (Korhonen *et al.*, 2011; Zhang *et al.*, 2014b) and organic solvents (Jiang and Hsieh, 2014b). There are several mechanisms involved in adsorption including complexation, ion exchange, microprecipitation and surface adsorption and all of these have been reported for cellulose-based adsorbents (Hokkanen, Bhatnagar and Sillanpää, 2016). Adsorption is also dependent on many characteristics of the water that is being treated such as pH, temperature and presence of other chemicals (Hokkanen, Bhatnagar and Sillanpää, 2016; Abouzeid *et al.*, 2019). Additionally factors such as adsorbent concentration, contact time and initial adsorbate concentration will affect the process (Abouzeid *et al.*, 2019).

2.3.2 Pressure-driven Membrane Separation

Membrane separation is an energy efficient method for removal of various different types of pollutants from water (Sharma *et al.*, 2020). Sustainability is considered one of the key requirements for future membrane materials (Nunes *et al.*, 2020), making nanocelluloses an interesting option for this application. In addition, the high strength, hydrophilicity and surface functionalization potential make cellulose nanomaterials a viable option for preparing separation membranes. Furthermore, the hydrophilicity and the controllable surface chemistry of nanocelluloses can reduce biofouling on the membrane surface (Voisin *et al.*, 2017; Lv *et al.*, 2018). The porosity, pore size and wet strength are important parameters that need to be considered when fabricating nanocellulose membranes. The low wet strength of cellulose nanopapers needs to be overcome to produce functional membrane materials. The pore characteristics typically determine the key performance parameters (the PWF and molecular-weight cut-off) of separation membranes. In terms of pore size, for instance *Cladophora* CNF has been used to produce membranes with tunable pore size, in the range of 10 to 25 nm, by altering the conditions of the hot-press drying of the filtered CNFs (Gustafsson and Mihranyan, 2016a). The water flux of membranes has also been enhanced by incorporating nanocellulose layers into membranes, for example by incorporating CNC into a polyamide skin layer (Wang *et al.*, 2017a) or into a PVDF membrane (Lv *et al.*, 2018).

BNC has been studied both in its as-synthesized (Hassan *et al.*, 2017) and mechanically disintegrated forms (Mautner *et al.*, 2015) for membrane separation. Vacuum filtering of CNF either incorporating membrane support materials (Visanko *et al.*, 2014; Soyekwo *et al.*, 2016; Cheng *et al.*, 2017; Wang *et al.*, 2019) or to produce self-standing nanopapers (Mautner *et al.* 2015; Metreveli *et al.*, 2014) has been used to produce CNF nanopaper membranes for size-exclusion based separation. Casting of CNF on different supports has also been used to produce membrane materials (Ma *et al.*, 2011, 2014; Kong *et al.*, 2014). Additionally, filters prepared from CNF by vacuum filtering and subsequent solvent exchange and freeze-drying or supercritical drying (Sehaqui *et al.*, 2016b) or dip coating with CNC (Karim *et al.*, 2016) have been reported. Furthermore, composites utilizing nanocelluloses have been produced for membrane separation (Varanasi, Low and Batchelor, 2015; Xu *et al.*, 2018). Due to its dimensions, CNF is suitable as barrier layers for microfiltration and ultrafiltration and for incorporation into matrix barrier layers for nanofiltration (Sharma *et al.*, 2020). The separation in the different cases introduced is typically based on size-exclusion, properties of the membrane such as hydrophilicity or hydrophobicity (Cheng *et al.*, 2017) or adsorption (Mautner *et al.*, 2016).

Applications demonstrated for nanocellulose filters include virus removal based on size-exclusion (Wang *et al.*, 2013; Metreveli *et al.*, 2014; Quellmalz and Mihranyan, 2015; Gustafsson *et al.*, 2016), oil-water separation based on the hydrophilicity (Hassan *et al.*, 2017; Cheng *et al.*, 2017; Galdino *et al.*, 2020) or hydrophobicity (Hou *et al.*, 2019) of the membrane, organic solvent separation (Mautner *et al.*, 2014), adsorption of heavy metals (Karim *et al.*, 2017; Mautner *et al.*, 2016) and desalination (Wang *et al.*, 2017a). Both functionalized and native cellulose nanomaterials have been used. Cross-linking using citric acid has been shown to be beneficial to achieve membranes with good wet strength (Quellmalz and Mihranyan, 2015). The focus of this section was on studies involving a pressure gradient as driving force but it should be noted that nanocellulose membranes can be suitable for separation applications involving other driving forces such as concentration, temperature and electric gradients (Sharma *et al.*, 2020). Examples of these include a forward osmosis membrane incorporating nanocellulose in the supporting layer (Cruz-Tato *et al.*, 2017) and bacterial nanocellulose films used as pervaporation membranes (Dubey *et al.*, 2002; Pandey, Saxena and Dubey, 2005).

2.3.3 Water Disinfection

The availability of microbially safe drinking water is a major concern in many areas of the world (Pradeep and Anshup, 2009). For water treatment in rural areas, point-of-use solutions provide a cheaper solution compared to water treatment infrastructure. There are several existing point-of-use technologies used for safe drinking water in remote areas, such as the LifeStraw and ceramic filters. However, issues such as high cost and inability to remove for instance viruses exist with these technologies (Sharma *et al.*, 2020). Silver is well known for its antibacterial properties and silver nanoparticles (AgNPs) have found growing interest in materials for water treatment (Chernousova and Epple, 2013). There are many studies that focus on functionalizing nanocellulose materials to introduce antibacterial properties, particularly involving AgNPs. Yet, most of these studies focus on biomedical applications. However,

solutions for water disinfection utilizing nanocellulose that are based on the separation techniques introduced in the previous sections, adsorption and membrane separation, have also been reported. Specifically filters for virus removal based on size-exclusion have been investigated in several studies, as discussed in the previous section. In addition to these, solutions involving antimicrobial surfaces or materials enabling the controlled release of antimicrobial agents can be considered. In the case of adsorption-based solutions and antibacterial surfaces, sufficient contact between the material and water needs to be ensured in order to achieve antibacterial effects. Wang *et al*. studied incorporation of CNC/zinc oxide nanorod clusters into aerogels and demonstrated significant decrease in bacteria concentrations when the material was added to water, due to the antibacterial activity of the zinc oxide clusters (Wang *et al*., 2017b). Suman *et al*. showed that nanocellulose composite pebbles containing AgNPs were effective for adsorptive water disinfection and, additionally, for heavy metal and dye removal (Suman *et al*., 2015). Chen and Peng reported a TO-CNF membrane incorporating AgNPs that had high water permeability and good water disinfection performance, ascribed to the antibacterial action of the AgNPs (Chen and Peng, 2017).

3. Materials and Methods

This section introduces the materials and methods used for the preparation of the nanocellulosic structures used in **Papers I-IV**. The characterization methods used and experiments conducted for testing the functionalities of the produced structures are also described.

3.1 Cellulose Nanofibrils and Preparation of Composites

The phosphorylated CNF (PHO-CNF) and TEMPO oxidized CNF (TO-CNF) used in **Paper I** and cationic CNF (cCNF) containing quaternary ammonium groups used in **Paper II** were received from Betulium Ltd., Finland. The concentrations of functional groups on the CNFs were provided by Betulium and were 1 mmol/g for the PHO-CNF, 1mmol/g for the TO-CNF and 0.63 mmol/g for the cCNF. Native CNF used as reference in **Paper I** was produced at Aalto University from bleached birch pulp using a microfluidizer (M110P, Microfluidics) with 200 and 100 μm chambers at 2000 bar and using 6 passes.

The cCNF containing composites for antibacterial studies were prepared by adding $Al_2(SO_4)_3$ solution (1.25 L, 0.5 M) dropwise to a dispersion of cCNF (1.5 L, 1.5 wt-%) and stirring the mixture for 3 h. For precipitation of the composite to occur, NaOH (2 M) was added to the mixture dropwise to reach pH 9 and the mixture was stirred for 1h. The precipitate was collected by vacuum filtering of the mixture and was washed with water. The precipitate was separated into two parts of which one was used for the composite without AgNPs (noted as cCNFAl) and the other for preparation of the composite containing silver (noted as $cCNFAl_{Ag}$). For embedding of AgNPs to the produced precipitate, 86 g of the precipitate was resuspended in 2 L of water and $AgNO_3$ (1.07 L, 5 mM) was added and the mixture was stirred for 1.5 h. $NaBH_4$ (1.07 L, 10 mM) was added dropwise at <10°C and stirring was continued for 20 min. The solution was left to stand for 20 min and then filtered to collect the precipitate and washed with water. For both cCNFAl and $cCNFAl_{Ag}$ the precipitates were dried to reach a solid content of 20-30 wt-% and then extruded through a syringe and dried.

3.2 Production of Bacterial Nanocellulose Structures

The BNC for the work presented in **Papers III** and **IV** was produced by the strain *Komagataeibacter medellinensis*, which was incubated at 28 °C. The strain, which was originally isolated from fruit vinegar in Colombia, was provided by Cristina Castro

from Universidad Pontificia Bolivariana, Colombia. Details of the strain have been reported by Castro *et al.* (Castro *et al.*, 2013). The growth medium consisted of 20 g/L glucose, 5 g/L of peptone, 5 g/L of yeast extract, and 2.5 g/L sodium diphosphate. The pH of the medium was adjusted to 4.5 with citric acid. The medium was sterilized either by autoclaving (120 °C for 20 min) or boiling for 15 min. The BNC pellicles for producing flat BNC membranes were grown in plastic containers by adding 2.5 L of sterilized medium to the containers and inoculating with 50 mL preculture (5, 7.5 and 10 days grown BNC) or 0.5 mL defrosted stock culture (14 days grown BNC). The formed pellicles were removed from the culture medium and first washed with DI water and then treated in 0.1 M NaOH at 60 °C for 4 h after which they were washed again with DI water (never-dried BNC, NDBNC). For dried BNC (DBNC) the pellicles were dried on a 50 °C hot plate and rewetted overnight in DI water before filtration tests or freeze-drying for SEM analysis. BNC-membranes with poly(oxyethylene) (POE) were produced by adding 10 g/L of 10 kDa POE into the culture medium and culturing for 10 days. BNC membranes treated with acetone were produced by immersing 10-day cultured BNC in acetone for 1 h and exchanging the acetone 2 times after which the BNC was left to dry in room temperature. The TEMPO oxidized BNC (TO-BNC) was produced using 14 days grown BNC and applying the conditions for TEMPO oxidation reported by Orelma *et al.* (Orelma *et al.*, 2014).

BNC capsules and complex 3D structures were produced utilizing polytetrafluoroethylene (PTFE) particles (size 35 μm) for stabilizing the air-medium interface. 80 mL of sterilized culture medium was inoculated with 1 mL of defrosted stock culture and grown for 2 days. For producing BNC capsules, a micropipette was used for applying drops of the medium precultured for 2 days on PTFE powder and incubating the produced, so-called liquid marbles, in humid conditions. Volumes of 10, 20, 30, 40, 50 and 60 μL were used. After given incubation times, the formed capsules were washed in water to remove PTFE particles and left in 0.1 M NaOH at room temperature for 24 h. The capsules were then washed with water to remove NaOH. The concept of liquid marbles has been introduced in literature (Aussillous and Quéré, 2001) and utilized for growing bacteria (Tian *et al.*, 2013). For encapsulation of functional cargo, a POE solution was used in addition to the culture medium and the preparation of the capsules containing encapsulated cargo is described in detail in section 3.8. For production of 3D structures, 3D printed PLA molds or 3 mL polystyrene cuvettes were used. The mold surfaces were modified with the PTFE particles by first partially dissolving the mold surfaces with acetone and then attaching the PTFE particles to the mold surfaces by vigorously shaking the molds after particle addition. After removing excess particles, the molds were filled with medium and incubated for given times. Cuboid shaped objects were produced by adding 1.5 mL of culture medium to the hydrophobized cuvettes and incubation for 3, 5 or 7 days.

3.3 Characterization Methods Used

A field emission scanning electron microscope (SEM) (Zeiss Sigma VP, Zeiss) was used for imaging of the samples. Before imaging the BNC and CNF samples were frozen at -80 °C and freeze-dried in a vacuum-dryer (FreeZone 2.5, Labconco). The samples were sputter coated with a 3 nm layer of platinum or platinum-palladium in order

to make the surface of the samples conductive and attached to aluminium stubs with carbon tape. The dry cCNFAl$_{Ag}$ composite was crushed into powder, sputtered with a 10 nm layer of gold and then attached to the carbon tape. An acceleration voltage of 1.6 kV was used for imaging. The energy dispersive X-ray (EDX) analysis of the cCNFAl$_{Ag}$ composite was conducted with a field-emission SEM with EDX (JSM-7500F, JEOL). The crushed samples were mounted onto copper tape on carbon stubs and then sputtered with a 10 nm layer of iridium. A nitrogen sorption measurement device (Tristar II, Micrometrics) was used for determining Brunauer-Emmett-Teller (BET) surface areas of composites.

A transmission electron microscope (TEM) (Technai 12, FEI) operated at 120 kV was used for imaging of the native and unmodified CNF. For preparation of the samples, a 3 µL drop of 0.01 wt-% CNF suspension was casted on a copper grid with an ultrathin carbon support film. After 1 min contact, excess solution was removed with filter paper and the samples were dried at room temperature. Then 3 µL of 2% uranyl acetate was used to stain the dried sample. The excess solution was again removed after 1 min contact time with filter paper and the sample was left to dry. For recording of FT-IR spectra, freeze dried samples of CNF were used. Spectra were recorded with 0.5 cm^{-1} intervals in the 400-4000 cm^{-1} region using a Fourier transform infrared (FT-IR) spectrometer (Nicolet 380 with ATR accessory, Thermo Fisher Scientific).

3.4 Adsorption of Uranium

All adsorption experiments were conducted at room temperature (21-22 °C). 5 mg in dry mass of the CNFs were used in 15 mL of solution for all experiments except for the selectivity study, where both 0.25 mg and 5 mg in 15 mL were used. Tests where different types of CNF were compared or pH varied were conducted using an initial uranium concentration of 100 ppm. Initial uranium concentrations of 10, 25, 50, 100, 200, 300, 400, and 500 ppm were used for adsorption isotherm studies. pH of the solutions was adjusted using 2 M HCl and NaOH and a pH of 6 was used for all studies excluding the study were pH was varied. For selectivity tests, initial concentrations of 10 ppm for each of the tested metals (U, Zn, Mn, and Cu) were used and other ions typically present in freshwaters were added according to the concentrations shown in Table S1 of Paper I. To start the tests, the suspensions containing CNF and uranium were sonicated in an ultrasonic bath at 37 kHz for 5 min and then left in a shaker at 200 rpm for 55 min. After this, 0.1 µm syringe filters were used to filter the samples and uranium concentration was analyzed at 651 nm spectrophotometrically with a microplate reader (Synergy H1, BioTek) using the Arsenazo III method reported by Khan *et al.* (Khan, Warwick and Evans, 2006). Further details of sample preparation for the spectrophotometric analysis are found in **Paper I**. Samples from the selectivity tests were analyzed with ICP-MS and were acidified by adding 5 vol-% of HNO_3 (68-70 %) before analysis. Control samples without CNF were used and analyzed for metal concentration for each test.

Experimental adsorption data from varying initial uranium concentration were used to calculate equilibrium adsorption capacities (q_e) according to equation 1. The data was fitted to Langmuir, Freundlich and Sips isotherm models, which are shown in equations 2, 3, and 4, respectively:

$$q_e = \frac{(C_0 - C_e)V}{m} \quad (1)$$

$$\frac{C_e}{q_e} = \frac{C_e}{q_{max}} + \frac{1}{q_{max}K_L} \quad (2)$$

$$\ln q_e = \ln K_F + \frac{1}{n}\ln C_e \quad (3)$$

$$\ln\left(\frac{q_e}{q_m - q_e}\right) = \frac{1}{n}\ln C_e + \ln K_s \quad (4)$$

Where C_o and C_e are the initial and equilibrium concentrations (ppm) of uranium, respectively, V is the volume (L) and m is the mass of adsorbent (g). For the isotherm models, q_{max} is the maximum adsorption capacity (mg/g), K_L and K_F are the Langmuir and Freundlich adsorption constants (L/mg), respectively, n is the dimensionless heterogeneity factor and K_s is the median association constant.

3.5 Characterization of Fibrils After Adsorption of Uranium

The samples for SEM imaging of PHO-CNF after uranium adsorption were taken from solutions after the CNF had been added to initial uranium concentrations of 50, 100, 250 and 500 ppm and sonication and shaking had been conducted as described in the previous section. 10 µL drops from these solutions were drop casted on carbon tape on an aluminium stub and freeze-drying was conducted as described previously. SEM imaging was done as described previously for BNC samples.

X-ray photoelectron spectroscopy (XPS) measurements were conducted with an electron spectrometer (AXIS Ultra, Kratos Analytical) with monochromatic A1 Kα irradiation at 100 W under neutralization using Whatman cellulose filter paper as reference. To prepare samples for XPS analysis, PHO-CNF was filtered onto 0.1 µm filters after batch adsorption of uranium, with initial uranium concentrations of 0, 100 and 500 ppm. The filter cakes were freeze-dried as described earlier for the SEM sample preparation. Three spots from each sample were analyzed and low-resolution survey scans were used for determination of elemental surface compositions. High resolution measurements were done for U 4f, C 1s and O 1s. Further details on XPS data analysis are found in **Paper I**.

3.6 Antibacterial Tests with Composites

Simulated freshwaters (Cl^-_{10ppm}, Cl^-_{90ppm} and Cl^-_{290ppm}) for use in antibacterial tests were prepared by dissolving different salts (NaCl, $MgSO_4$, KNO_3, $NaHCO_3$, and $CaCl_2$) in Milli-Q water to reach the concentrations presented in Table S1 of **Paper II**. The chloride concentrations were chosen based on chloride concentrations found in field water samples (refer to **Paper II** for more details). The natural drinking water composition used in the study of Sankar *et al.* (2013) was used as a basis for formulating the compositions of the simulated freshwaters. $Cl^-_{120ppm+nutrient}$ water occurred in tests where bacteria were inoculated together with the culture medium into the Cl^-_{90ppm} water, resulting in higher sodium and chloride concentrations.

For antibacterial tests, the strains used were *Escherichia coli* (DSM 1116, ATCC 9637) and *Bacillus subtilis* (1012M15). Simulated freshwaters were filtered with 0.2 µm sterile syringe filters and all used glassware were sterilized by autoclaving. 250 mL Erlenmeyer flasks containing a total volume of 50 mL of simulated freshwater were used. $cCNFAl_{Ag}$ was used at a concentration of 4 g/L and controls without composite were used for each test. For preparation of precultures, 4 mL of Luria Bertani (LB) medium was inoculated with the bacteria and incubation was conducted overnight under 220 rpm and at 37 °C and 30 °C for *E. coli* and *B. subtilis*, respectively. For tests comparing the antibacterial activity on the two strains, an inoculum of 0.5 mL (diluted with LB medium) was added to 49.5 mL of Cl^-_{90ppm} simulated freshwater to reach starting bacterial concentrations between 10^6 and 10^7 CFU (colony forming units)/mL. For tests comparing the antibacterial effect on *E. coli* with varying chloride concentration, 0.2 mL of the preculture was centrifuged (2 min, 5000 rcf) and after carefully removing the medium the cells were suspended in 0.5 mL of the simulated freshwaters and the centrifugation was repeated. Finally, the cells were resuspended in a total volume of 50 mL of the simulated freshwaters. For all the tests, flasks were incubated at 100 rpm at 37°C or 30°C for *E. coli* and *B. subtilis*, respectively. After incubation, 50 µL of sample (necessary dilutions to achieve countable amounts of colonies were conducted with the simulated freshwaters) was evenly spread on LB agar plates that were incubated overnight. The number of colonies was calculated as an average from three parallel plates.

The Ag release from the $cCNFAl_{Ag}$ composite was determined in Cl^-_{90ppm} and $Cl^-_{120ppm+nutrient}$ simulated freshwaters by incubating flasks containing 50 mL of the waters and 4 g/L of the composite at 37 °C and 100 rpm. Ag concentrations were analyzed by inductively coupled plasma mass spectrometry (ICP-MS) (NexION 300X, PerkinElmer) from samples taken at 15, 30, 60, 120, and 24 h from the start of the tests. Before analysis, 5 vol-% of HNO_3 (68-70 %) was added to the samples.

3.7 Filtration Studies with Bacterial Nanocellulose

Before conducting filtration tests the dried membranes were rehydrated in DI water for at least 12 h. For majority of the filtration experiments, a cross-flow filtration unit (CF042, Sterlitech corporation) with an active membrane area of 42 cm^2 was used. For experiments with bovine serum albumin (BSA), a dead-end stirred cell (Amicon 8200, Millipore) with an active membrane area of 28.7 cm^2 was used. Schematics of the filtration units used are shown in Figure 5. Milli-Q water was used for preparing the solutions containing solute and for PWF determination. For experiments with the cross-flow unit, the membranes were compacted at a pressure of 2.5 bar for 30 min after which tests were conducted at a pressure of 2 bar and run for at least 1 h. For the experiments investigating flux hysteresis, the operating pressure was increased stepwise to 2.5 bar (0.25, 0.5, 1, 1.5, 2 and 2.5 bar) and then decreased stepwise using the same pressures. PWFs were determined 30 min after each pressure change. Results were calculated as an average from the repeats. The concentration used for POE solutions was 1 g/L. When conducting tests with the POEs, both permeate and concentrate flows were directed back to the feed before starting sample collection. The tests were completed as a consecutive sequence with the same BNC membrane in the order of

increasing POE molecular weight (0.1 MDa, 0.4 MDa, 1 MDa and 2 MDa) and the system was cleaned thoroughly in between runs. Tests were repeated at least three times using a new membrane for each experiment. A total organic carbon (TOC) analyzer (TOC-VCPH, Shimadzu) was used to determine permeate and feed concentrations. For BSA filtration experiments at different pH, the stirred cell was pressurized with compressed air to 2 bar. BSA was dissolved at a concentration of 0.5 g/L in either phosphate buffered saline (PBS) (pH 7.4) or 50 mM sodium acetate buffer (pH 4, 5 and 6). Experiments were started with the pH 7.4 solution and continued in order of decreasing pH. The BNC membrane was washed with DI water after the experiment with each solution. The series of experiments was conducted twice for each set of BNC membranes. A UV-Vis spectrophotometer (UV-2550, Shimadzu) was used for measuring absorbance of permeate samples at 280 nm to determine BSA concentrations. Equation 5 was used to determine PWF (J) and Equation 6 to determine rejections

$$J = \frac{V}{A\Delta t} \quad (5)$$

$$R(\%) = \frac{C_f - C_p}{C_f} x100\% \quad (6)$$

where V is the volume of permeate (L), A is the membrane surface area (m^2), Δt (h) is the time used for collecting sample, C_f is the feed concentration and C_p is the permeate concentration.

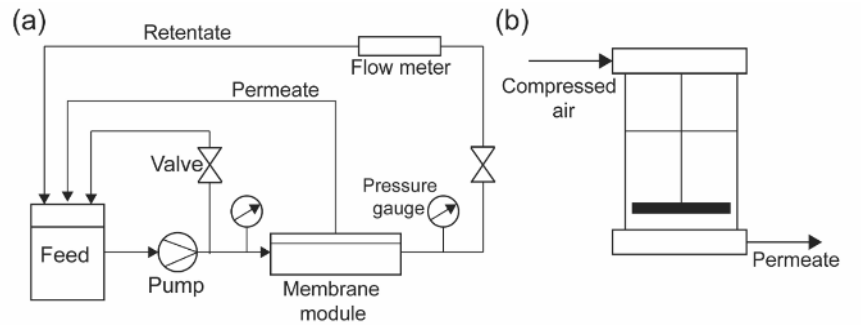

Figure 5. Schematics of the (a) cross-flow and (b) dead-end units used for the filtration studies with bacterial nanocellulose membranes. (**Paper III**)

3.8 Functionalities of 3D structures

For gravimetric analysis, the capsules were first freeze-dried and then weighed with a balance (MT5, Mettler Toledo) having an accuracy of 0.001 mg. The details for synthesis of the gold nanoparticles (AuNPs), FITC labelled chitosan and metal organic framework encapsulated horseradish peroxidase (MOF-HRP) are found in **Paper IV**. For encapsulation of the different cargo, a 20 wt-% solution of 2 kDa POE was mixed with the culture medium that had been incubated for 2 days in a ratio of 1:1. Then between 5 to 25 µL of suspension containing cargo was added to 35 µL of the mixture of POE and medium and mixed to evenly distribute the cargo (final cargo concentrations were between 5 and 0.5%). The chitosan and MOF-HRP containing capsules

were incubated for 4 days and the AuNP containing capsules for 2 days. For the MOF-HRP containing capsules, a higher pH when incubating the capsules was needed in order to prevent the degradation of the enzyme and MOF architecture. A pH of 6.85 was used, since at this pH, robust capsules were formed and the MOF-HRP exhibited significant activity. For evaluating enzymatic activity in the capsules, the capsules were added to 3 mL of 50 mM sodium phosphate buffer (pH 7) for measuring the baseline and then 20 µL of *o*-dianisidine (5 mg/mL) was added and the solution was mixed. After this, 0.5 µL of hydrogen peroxide was added and the solution was mixed again. The UV absorbances were measured at 440 nm at given times and averages of three measurements from individual capsules were used to plot the curves. The UV-absorbance spectra for the capsules containing cargo and controls were measured using a Shimadzu UV-2550 spectrophotometer. For tensile testing of the cuboid shaped objects, the shapes were first compressed laterally to a thickness of 0.9 mm. A universal tensile tester (Instron 4204, Instron) with a loading rate of 20 mm min^{-1} was used. The distance between clamps was 5 mm. The results are reported as an average of three measurements.

4. Results and Discussion

This section provides a summary of the main findings of **Papers I-IV**. A more detailed description of the results is found in the papers attached.

4.1 Studies Utilizing Cellulose Nanofibrils

4.1.1 Characterization of Cellulose Nanofibrils

Native CNF, cCNF, TO-CNF, and PHO-CNF were used in this work. These materials were characterized by TEM and FT-IR spectroscopy (Figure 6). TEM images indicated the fibrillar structure of the CNFs, with native CNF having much longer fibrils compared to the modified CNFs. The FT-IR spectra confirmed the presence of functional groups on the modified CNFs. Characteristic bands for cellulose were observed in all samples (peaks at around 1030 and 2900 cm^{-1} attributed to the C-O and C-H stretching vibrations, a peak at around 1640 cm^{-1} attributed to the O-H bending of adsorbed water and a broad band at 3340 cm^{-1} corresponding to O-H stretching vibrations). Peaks at around 820 cm^{-1}, 930 cm^{-1} and 1230 cm^{-1}, which corresponded to P-O-C, P-OH and P=O stretching vibrations, respectively, were observed in the PHO-CNF sample. A peak at around 1600 cm^{-1} observed for the TO-CNF was attributed to the C=O stretching vibration of the COO^- group. For cCNF, a peak was observed at 1480 cm^{-1}, corresponding to the methyl group of the quaternary ammonium units.

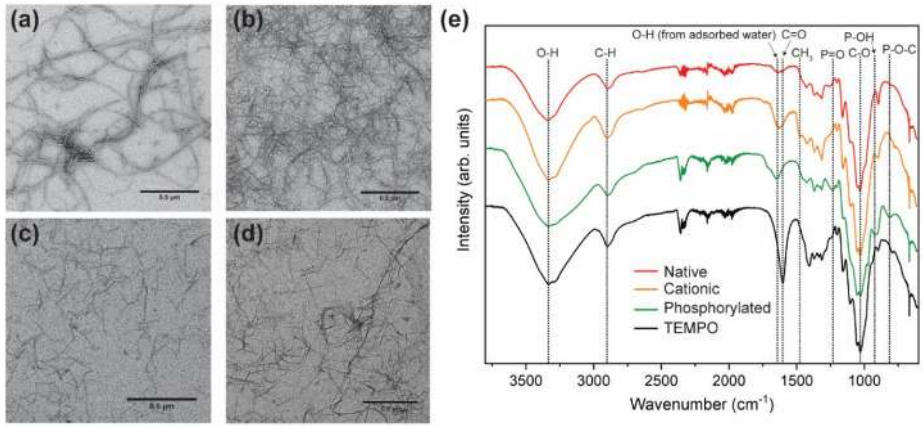

Figure 6. TEM images of (a) unmodified, (b) TEMPO oxidized, (c) phosphorylated and (d) cationic CNF. Scale bars are 0.5 μm. (e) FT-IR spectra of the CNFs. (**Papers I** and **II**)

4.1.2 Uranium Adsorption

Under aerobic conditions, uranium is typically present in water in its hexavalent form as the uranyl ion (UO_2^{2+}) (Sylwester, Hudson and Allen, 2000). Depending on the pH and other ions present in the solution, different types of UO_2^{2+} complexes are formed (Berto *et al.*, 2012; Xie *et al.*, 2019). Materials containing phosphorous based functional groups have been shown to favor the binding of UO_2^{2+} species through chelation (Xie *et al.*, 2019). Batch adsorption studies were conducted to study the removal of uranium with PHO-CNF (1 mmol/g) with varying initial uranium concentration. SEM and XPS analysis were conducted on the fibrils after uranium adsorption for insights on the adsorption process. SEM images gave evidence of fibril aggregation occurring when initial uranium concentration was increased (Figure 7a-c). When the initial concentration was 100 ppm, fibrillar morphology could still be observed but with initial uranium concentration of 250 ppm and 500 ppm, sheet-like morphology was evident from the images. The presence of uranium on the fibrils after adsorption was confirmed by XPS results based on the position of the $U4f_{7/2}$ peak, which was detected for both 100 ppm and 500 ppm samples (Figure 7d). XPS results also indicated decrease in the amount of sodium in the samples, as uranium concentration increased. Since sodium was present on the PHO-CNF as counterion of the phosphoryl groups, this could be an indication of the occurrence of ion-exchange when uranium was adsorbed on the fibrils. An interesting observation that was made from the batch adsorption experiments was that when initial uranium concentrations were high, a gelling effect of the PHO-CNFs could be observed (Fig. 7e). From the sample with initial uranium concentration of 500 ppm, this could clearly be observed. This provided further indication of a crosslinking mechanism occuring between the PHO-CNFs and the uranyl or uranyl complex ions, which led to hydrogelation of the fibrils as a result of reduction of the electrostatic repulsion between the fibrils.

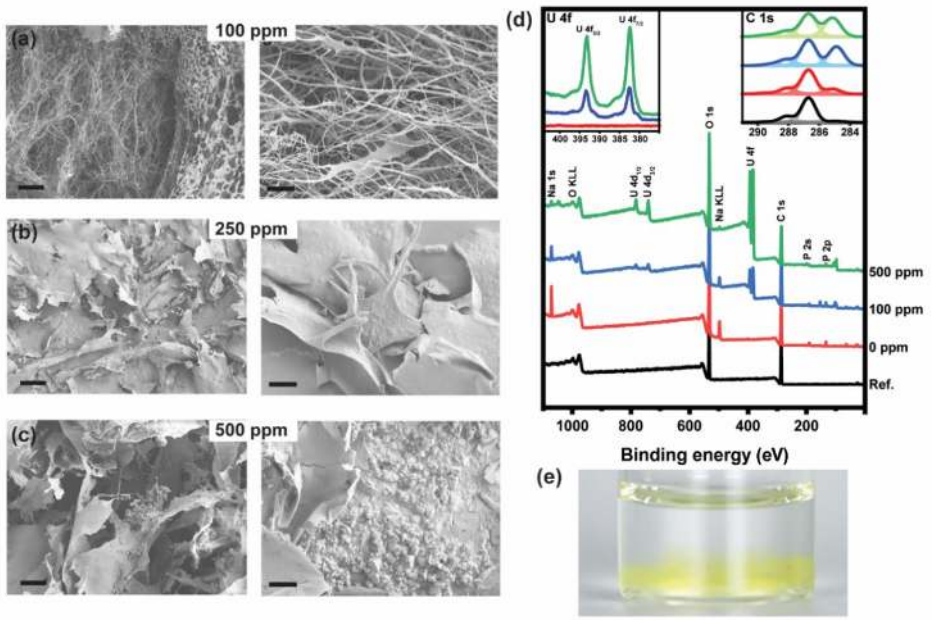

Figure 7. SEM images of PHO-CNF (1 mmol/g) after 1 h contact with solutions of initial uranium concentrations of (a) 100 ppm (b) 250 ppm and (c) 500 ppm. The scale bars for all the SEM images are 20 μm (left) and 3 μm (right). (d) Survey spectra from XPS measurements of reference cellulose sample and PHO-CNF (1 mmol/g) after uranium adsorption from initial concentrations of 0 ppm, 100 ppm and 500 ppm. High-resolution U 4f and C 1s spectra are depicted in the insets. (e) Gelling effect observed with PHO-CNF when initial uranium concentration was 500 ppm. (**Paper I**)

Batch adsorption studies to compare the adsorption of uranium on PHO-CNF to TO-CNF and native CNF were also conducted (Figure 8a). Among these samples, the PHO-CNF was found to clearly exhibit the highest percentage of uranium removal (94%) compared to TO-CNF (77%) and native CNF (7%). Both the high anionic charge and smaller size of the PHO-CNF and TO-CNF compared to native CNF could explain the higher removal percentages. The higher removal percentage of PHO-CNF compared to TO-CNF indicated that phosphoryl groups had higher affinity to the UO_2^{2+} species present compared to the carboxyl groups of the TO-CNF. The effect of pH on the uranium removal capacity in the pH range 3-7 was studied with PHO-CNF (Figure 8b). The removal capacity was not significantly affected by pH between 3-6 but at pH 7 a 30 % reduction in removal was observed. This was mainly ascribed to the formation of neutral and anionic UO_2^{2+} complexes at pH above 5. When varying initial uranium concentration (Figure 8c), the experimental data were fitted to Langmuir, Freundlich and Sips isotherm models. The best fit was found with the Sips isotherm model. A maximum adsorption capacity of 1550 mg/g was calculated based on this model. This value is higher than values reported in literature for uranium adsorption by other bioadsorbents, including carboxycellulose nanofibers with a q_{max} of 1467 mg/g (Sharma *et al.*, 2017) and phosphorylated cactus fibers with a q_{max} of 107 mg/g (Prodromou and Pashalidis, 2013). In addition to high adsorption capacity, the

selectivity of the adsorbent to uranium over other metals and ions present in the water can be a key factor depending on the intended application. The selectivity of PHO-CNF against other metals (Cu, Zn and Mn) and ions typically present in freshwaters were studied (Figure 8d). Based on these results, the removal percentages for uranium were the highest compared to the other metals studied and the other ions present in the water (Cl^-, SO_4^{2-}, NO_3^-, carbonates, Na^+, Mg^{2+}, K^+ and Ca^{2+}) did not influence the removal of uranium. When the PHO-CNF amount was decreased to 0.25 mg in 15 mL of solution, the high selectivity to uranium was evident. To conclude, the batch adsorption studies and analysis methods used in studying the adsorption of uranium to PHO-CNF gave clear indication that PHO-CNF can remove uranium with high adsorption capacity and selectivity and therefore has potential to be applied as a bioadsorbent for uranium removal from highly contaminated waters.

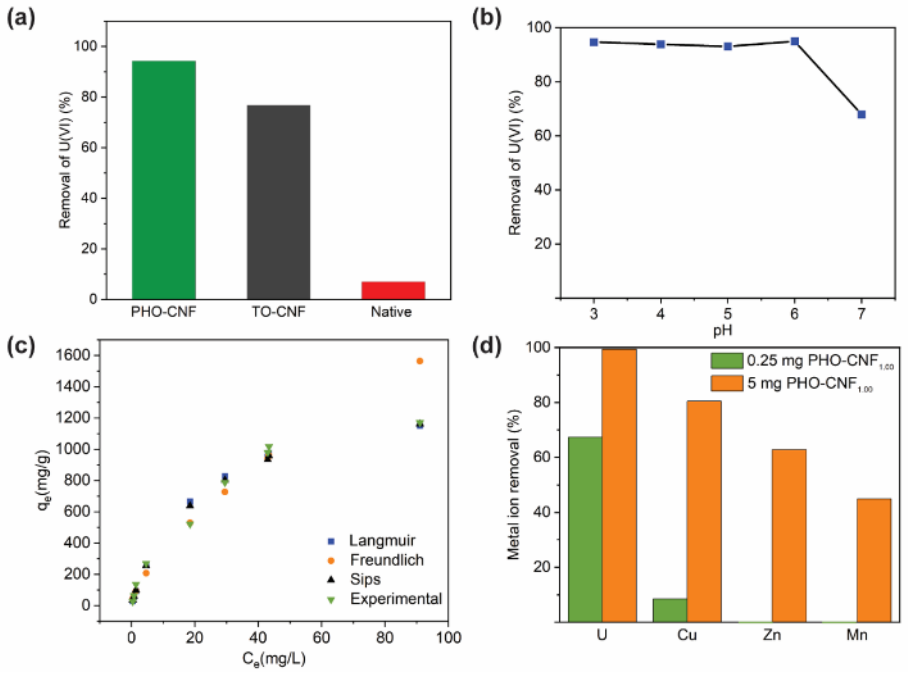

Figure 8. Results from batch adsorption studies of uranium. (a) Comparison of uranium removal using PHO-CNF, TO-CNF and native CNF. (b) Effect of pH on removal of uranium with PHO-CNF. (c) Effect of initial uranium concentration. The experimental adsorption data compared to data fitted to Langmuir, Freundlich and Sips isotherm models. (d) Selectivity of PHO-CNF to uranium against Cu, Zn and Mn. (**Paper I**)

4.1.3 Antibacterial Activity of the Composites

A granular composite material with efficient antibacterial activity composed of chitosan and aluminium oxyhydroxide embedded with AgNPs has previously been reported (Sankar *et al.*, 2013). Taking inspiration from this work, a composite material utilizing cCNF instead of chitosan was developed (cCNFAl$_{Ag}$). Cationic fibrils were used instead of native CNF due to the inherent antibacterial properties of cCNF

(Chaker and Boufi, 2015). The $cCNFAl_{Ag}$ composite was characterized by SEM, SEM-EDX elemental mapping and BET measurements, and the silver release from the composites was analyzed (Figure 9). The SEM image (Figure 9a) indicated that the composite had a porous structure. The BET surface area of the composite was 150 m^2/g, which further supported the observation from the SEM image. SEM-EDX mapping (Figure 9c) confirmed the presence of silver in the composites. The measurements on silver release from the composites (Figure 9b) indicated that the silver release was time dependent but saturated after 24 h contact time in both of the simulated freshwaters used for the experiments (Cl^-_{90ppm} and $Cl^-_{120ppm+nutrient}$). The saturation point for both of the simulated freshwaters was below 100 ppm, which is the health advisory lifetime maximum level of silver reported by the United States Environmental Protection Agency (U.S. Environmental Protection Agency, 2012). It was also observed that a contact time of approximately 1 h was needed in both simulated freshwaters to achieve a silver concentration above 50 ppm, which has been reported as the concentration needed to achieve sufficient antibacterial effect in typical natural freshwaters (Swathy *et al.*, 2014). However, it should be noted that the silver concentrations released from the material are also dependent on the concentration of the material used and if higher concentrations were used, shorter contact times would likely be sufficient to achieve a 50 ppm silver concentration. The concentrations reported here were the total concentrations of silver in dissolved silver species present in the waters and it should be considered that the antibacterial effect is mainly attributed to the concentration of free silver ions (Ag^+) present in the waters (Chernousova and Epple, 2013; Levard *et al.*, 2013a). The percentages of Ag^+ of the total silver concentrations were determined by computational speciation analysis (using PHREEQC software) for the simulated freshwaters used for antibacterial tests with *E. coli*. The calculated percentages were 64.9, 15.3 and 3.9 for the Cl^-_{10ppm}, Cl^-_{90ppm} and Cl^-_{290ppm} simulated freshwaters, respectively, clearly indicating the effect of chloride concentration on the availability of Ag^+.

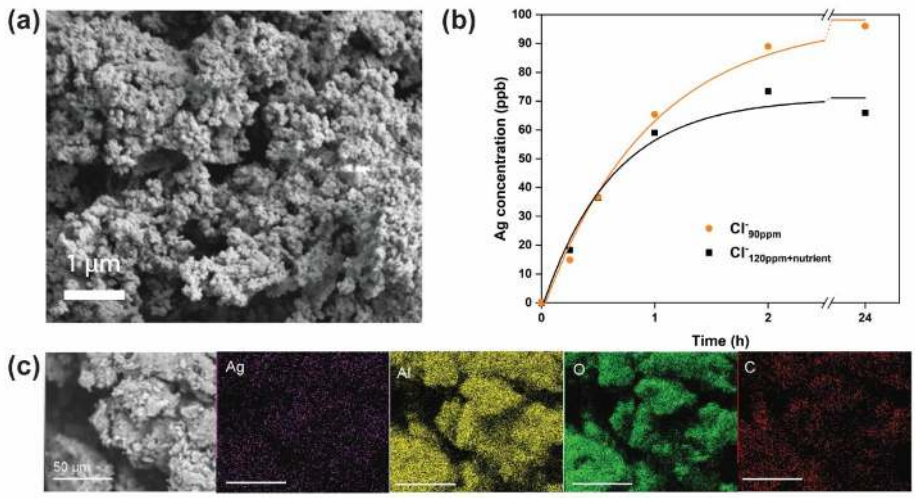

Figure 9. Characterization of $cCNFAl_{Ag}$ composite. (a) SEM image of $cCNFAl_{Ag}$ composite. (b) Silver release from the composite at a concentration of 4 g/L in Cl^-_{90ppm} and $Cl^-_{120ppm+nutrient}$ simulated freshwaters. The exponential decay curves have been plotted to guide the eye. (c) SEM-EDX elemental mapping of $cCNFAl_{Ag}$ composite (all scale bars are 50 µm). (**Paper II**)

The antibacterial activity of the composite on *E. coli* and *B. subtilis* was compared (Figure 10a). For the tests, simulated freshwater containing 1% of LB medium was used ($Cl^-_{120ppm+nutrient}$). The small amount of LB was needed to ensure the viability of *B. subtilis* for the duration of the tests. These tests indicated that the composite had efficient antibacterial activity on *B. subtilis* since a decrease of 6.6 $\log_{10}$ in bacterial count was observed after 2h. The presence of nutrient in the simulated freshwater led to bacteria growth in the control samples. This in addition to the potential complexation of Ag^+ with the components of LB, were likely the reasons for low antibacterial activity against *E. coli*. Further tests were continued with *E. coli* with simulated freshwaters without LB (Figure 10b), since in natural waters, concentrations of appropriate nutrients for bacterial growth are typically low (Jannasch, 1969). Three simulated freshwaters with varying chloride concentrations were used (Cl^-_{10ppm}, Cl^-_{90ppm} and Cl^-_{290ppm}), because chloride concentration can vary significantly in natural freshwaters from different sources. Chloride can reduce the antibacterial effect of Ag^+ due to complexation (Levard *et al.*, 2013b; Swathy *et al.*, 2014). Contact times of 1 h and 2 h were used and based on the results the 2 h contact time was enough to kill all bacteria in each of the simulated waters. However, at 1 h contact time, significant differences could be observed, indicating that chloride concentration influences the antibacterial activity. When the chloride concentration was 10 ppm, a 5.6 $\log_{10}$ reduction was observed, whereas when the chloride concentration was 90 ppm, only a 2.9 $\log_{10}$ decrease was observed. It should be noted that the initial bacteria concentrations used in this study were high compared to concentrations typically present in natural drinking waters. Therefore, it is expected that shorter contact times could be used in real life applications. Based on the antibacterial studies, the $cCNFAl_{Ag}$ composite presents good antibacterial effect when chloride concentration is low. If chloride

concentrations are high, it should be ensured that the contact time is long enough to achieve sufficient antibacterial effect.

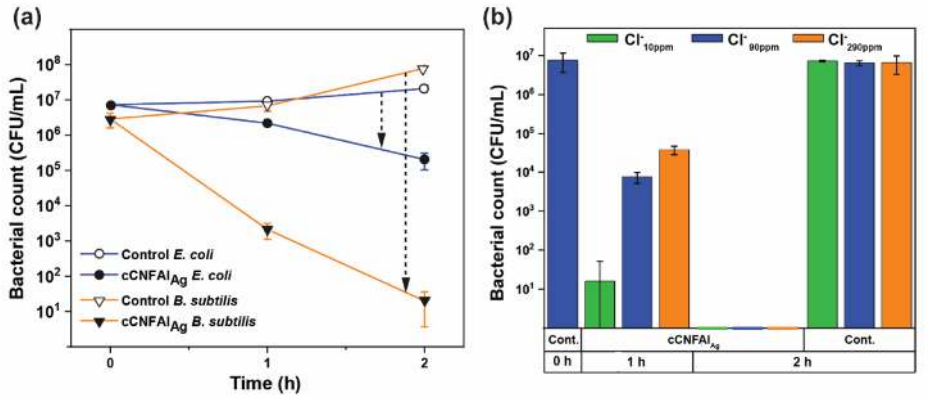

Figure 10. Results from antibacterial tests with cCNFAl$_{Ag}$ composites. (a) Antibacterial effect against *E. coli* and *B. subtilis* in Cl$^-_{120ppm+nutrient}$ simulated freshwater. (b) Antibacterial effect of the composite against *E. coli* in simulated freshwaters with varying chloride concentration. (**Paper II**)

4.2 Studies with Bacterial Nanocellulose

4.2.1 Pressure-driven Filtration with Bacterial Nanocellulose

BNC membranes grown in static cultures were investigated for their use as separation membranes in a pressure-driven unit. The filtration properties of BNC depend on the cultivation conditions, the pre-compression of the network or other post-cultivation treatment and the processing variables used in the separation process. The influence of pressure up to 2.5 bar and the effect of drying induced compression on the behavior of the membranes in terms of PWFs was first studied (Figure 11a). NDBNC and DBNC showed a clear difference in the PWFs and their behavior under pressure. For NDBNC, the fluxes are significantly higher (89 % higher flux at 2.5 bar compared to DBNC), but flux hysteresis is observed as the pressure is decreased, indicating significant densification of the NDBNC network structure when pressure is applied. For DBNC, no significant flux hysteresis was observed, which was indication of the significant drying induced conformational changes that had occurred in the DBNC. A further indication of the densification of the NDBNC network upon pressure increase was the faster increase of PWF with pressure for DBNC compared to NDBNC (an increase of 39% in PWF from 1 to 2 bar for DBNC was observed compared to 24% for NDBNC).

The rejections and fluxes of a series of POEs of varying average molecular weight were also determined for both NDBNC and DBNC (Figure 11b). The hydrodynamic radii for the POEs used were estimated to be 10 nm, 20 nm, 40 nm and 60 nm corresponding to the average molecular weights 0.1 MDa, 0.4 MDa, 1 MDa and 2 MDa, respectively. For NDBNC, a plateau in the rejection was reached at 0.4 MDa, whereas for the DBNC a plateau was observed at 1 MDa. The rejections were higher for the

DBNC compared to NDBNC, which was expected due to the pre-compressed structure of DBNC. For both NDBNC and DBNC, a significant decrease in POE flux occurred from 0.1 MDa POE to 0.4 MDa POE (93% for NDBNC and 65% for DBNC). This indicated that adsorption of 0.4 MDa POE caused significant pore clogging for both NDBNC and DBNC.

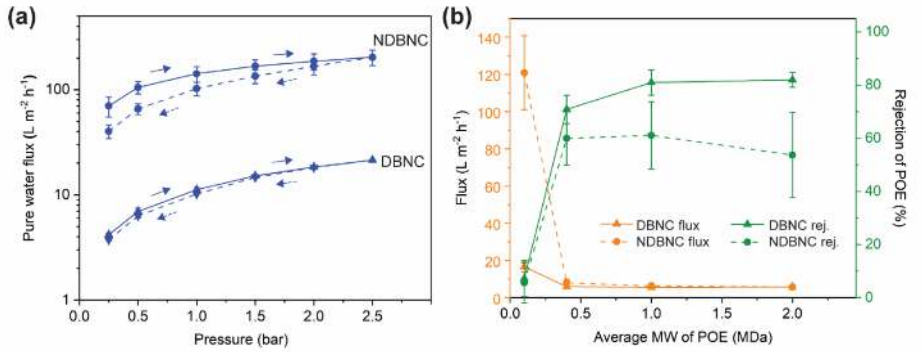

Figure 11. Comparison of filtration properties of never-dried BNC (NDBNC) and dried BNC (DBNC). (a) Influence of pressure on the PWF of NDBNC and DBNC and flux hysteresis. (b) Rejections and fluxes of different size POEs with NDBNC and DBNC at an operating pressure of 2 bar. (**Paper III**)

The influence of culture conditions (incubation time and addition of 10 kDa POE to culture medium) and post-culture solvent treatment with acetone was studied for DBNC. SEM images of BNC incubated for 10 days indicated that compared to unmodified BNC (Figure 12a), acetone treatment before drying (Figure 12b) led to a more porous surface structure, whereas addition of POE to the culture medium (Figure 12c) resulted in a slightly denser surface structure. To compare the behavior of the BNC membranes in the wet state and under pressure, filtration properties of the membranes were tested. First the impact of incubation time on the filtration properties was studied (Figure 12d). The PWF was 69% lower for the 10 days grown BNC compared to 5 days grown BNC at 2 bar pressure and as expected, rejections for 0.1 MDa POE and 0.4 MDa POE were lower for the 5 days grown BNC compared to the 10 days grown BNC. When the membranes grown for 10 days were treated with acetone before drying (BNC-ac), the flux increased by 59% and when POE had been added to the culture medium the flux decreased by 51%. As expected, the opposite trend was observed for the rejections of 0.1 MDa POE and 0.4 MDa POE. These results indicated a more porous structure of the BNC-ac membrane and a densified structure of the BNC-POE membrane when compared to the unmodified BNC membrane. Overall, these results indicate that there are various ways to modify the BNC network structure and consequently its filtration properties.

The effect of BNC surface charge on the separation of BSA, used here as a model protein, was also investigated using a negatively charged TO-BNC membrane (Figure 12e). It should be noted that PWF was 54% lower for the TO-BNC compared to unmodified BNC. Based on the results, it could be seen that the solution pH had a significant impact on the separation of BSA. BSA is negatively charged when the pH is above its isoelectric point (4.7) and positively charged when the pH is below this point.

The highest rejections where achieved at pH 4 and 5, where nearly complete rejection of BSA was achieved. Particularly at pH 4, the high rejection could be attributed to the formation of BSA aggregates, since at this pH the membrane and BSA are oppositely charged. However, rejections at pH 6 and 7.4 were also higher for the charged BNC membrane compared to unmodified BNC, which could possibly be caused by a repulsion effect of the negatively charged membrane towards the negatively charged BSA. Based on these results, it is concluded that even though based on the principle of size-exclusion, BNC membranes are permeable to most proteins, separation based on affinity is possible by tuning the solution pH and BNC surface charge. The next section presents the extension of BNC production from 2D pellicles studied in this section to controlled fabrication of more complex structures to broaden the application range beyond the possibilities provided by flat sheet BNC membranes.

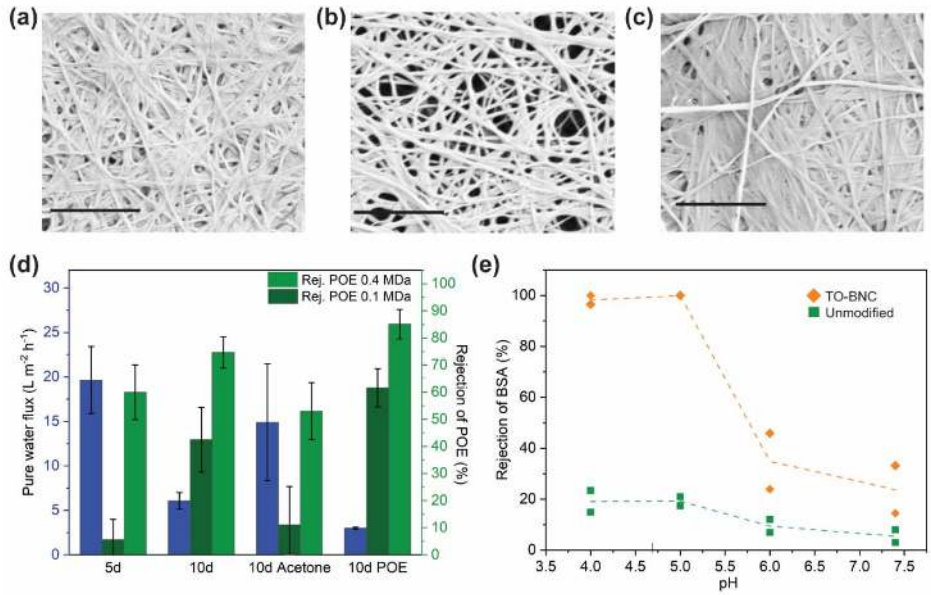

Figure 12. SEM images of 10 days grown (a) unmodified BNC (b) acetone-treated BNC and (c) BNC incubated with POE added to culture medium. (d) Effect of growth time and modification on the PWFs and rejections of POE with average molecular weights 0.1 MDa and 0.4 MDa. (e) Effect of introducing negative surface charge on BNC by TEMPO oxidation on the rejection of BSA at pH 4, 5, 6 and 7.4. Results from individual experiments are indicated by the points and dashed lines are an indication of the trend in the rejection values. The filtration tests were conducted at 2 bar pressure. (**Paper III**)

4.2.2 Biofabrication of Nanocellulosic 3D Structures

The concept of liquid marbles and the "drop-cast" method was utilized to produce hollow capsules of BNC (Figure 13). The PTFE particles stabilized the interface of the culture medium and air and the size of the capsules could be controlled by the liquid marble volume. The produced capsules were found to replicate the shape of the liquid marble (Figure 13a). SEM imaging revealed the typical BNC fiber network structure

and porous morphology of the capsule surface. The dry weight of the capsules was found to increase with increasing marble volume but in the case of increasing incubation time, the dry weight plateaued already at 2 to 4 day incubation time, depending slightly on the initial marble volume (Figure 13b). This indicated fast growth rate during the first days of incubation, which was likely a result of the good oxygen access for the bacteria at the surface of the liquid marbles. When the incubation time was fixed to 4 days, a linear increase was observed in the mass of BNC that was produced when initial marble volume was increased (Figure 13c).

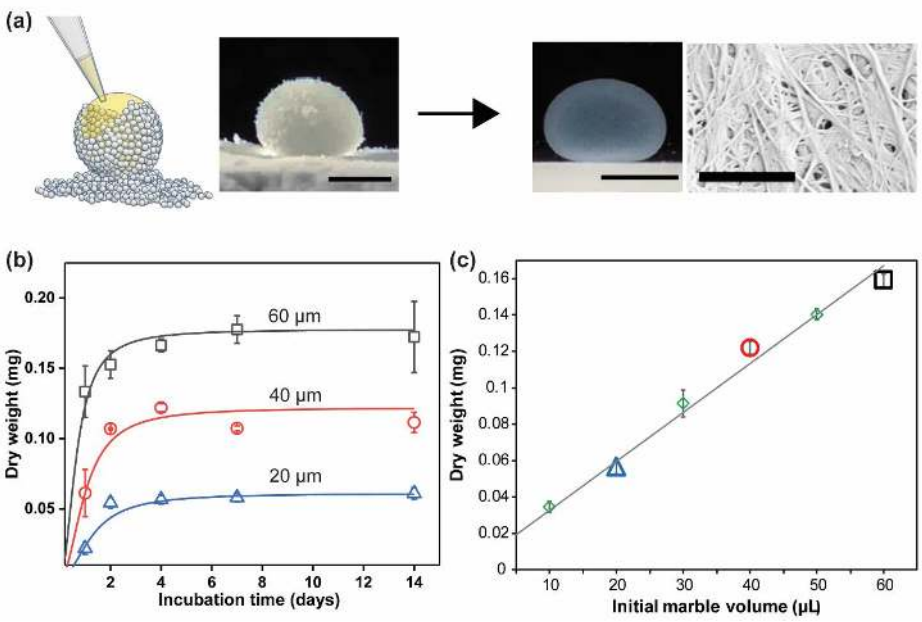

Figure 13. (a) Production of hollow capsules using the drop cast technique and utilizing hydrophobic PTFE particles. Images of the liquid marble produced using 40 µL of culture medium and the corresponding capsule produced after incubation are shown. The surface morphology of the produced capsule is shown in the SEM image. Scale bars are 3 mm for the photos and 1 µm for the SEM image. (b) Dependence of dry weight of capsule on incubation time for 20, 40 and 60 µL capsules. (c) Dry weight of BNC as a function of initial marble volume for capsules grown for 4 days. (**Paper IV**)

The potential of introducing functionalities to the capsules was investigated by the in situ encapsulation of different particles and polymers inside the capsules (Figure 14). To prevent aggregation when the different cargos were added to the culture medium, POE was used to reduce the interactions between the cargo and medium. It was demonstrated that a particulated enzyme, namely HRP encased into a MOF, could be successfully encapsulated. The activity of the encapsulated enzyme was demonstrated and although the activity reduced at increased temperature (100 °C), significant activity could still be detected. Encasing the enzyme in the MOF provided temperature and solvent resistivity, which corresponds well with the properties of the BNC capsule.

The encapsulation of FITC-labelled chitosan (Figure 14b) and AuNPs (Figure 14c) was also demonstrated. For the FITC-chitosan containing capsule, a shift in the wavelength of maximum absorption was observed as a function of pH, which suggested potential for development of pH responsive sensors. The AuNPs have potential for use in plasmonic heating (Neumann *et al.*, 2013), thus making the BNC capsules ideal for their encapsulation due to the thermal resistance of BNC. The AuNPs were successfully loaded into the capsules but were found to have significant interaction with the capsule shell, since a shift in their absorbance was observed when encapsulated. Based on the studies conducted, the BNC capsules containing functional cargo or functionalities in the shell could be envisioned to have potential for different types of in-water applications, such as plasmonic heating, sensing or use as an enzymatic reactor.

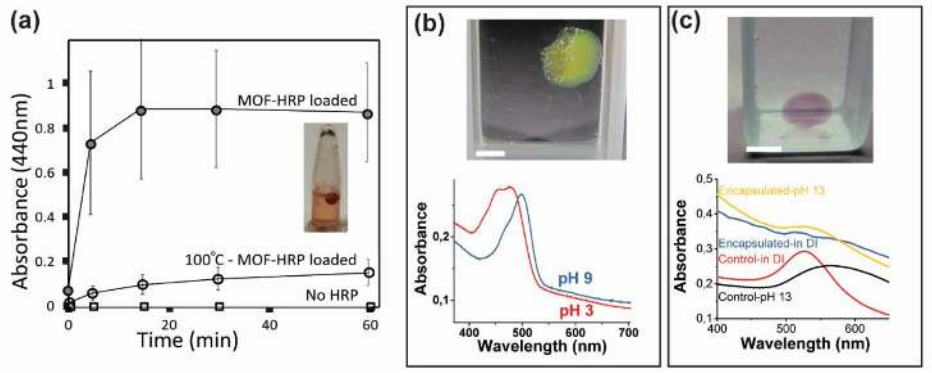

Figure 14. Encapsulation to introduce functional cargo into biofabricated capsules. (a) Encapsulation of MOF protected HRP and catalytic conversion of o-dianisidine. (b) Encapsulation of FITC-chitosan and UV-Vis absorption spectra at pH 3 and 9. (c) Encapsulation of gold nanoparticles and UV-Vis absorption spectra at pH 13 and in DI water. The control indicates the absorption of the gold nanoparticle suspension. (**Paper IV**)

More complex BNC structures, such as an ear shape, with sizes up to several centimeters were produced using PLA molds superhydrophobized by embedded PTFE particles (Figure 15a). The particles embedded in the mold surface enabled oxygen access to the interface between the culture medium and the mold, leading to replication of the mold structure with micron scale fidelity. Cuboids were produced by using superhydrophobized polystyrene cuvettes and the mechanical properties of cuboids with different incubation times were tested (Figure 15b). The maximum tensile load for cuboids that had been incubated for 3 days was much lower compared to cuboids incubated for 5 or 7 days. This indicates the possibility to tune the mechanical properties of the produced materials by varying the incubation time. To summarize, the new technique presented here for the facile production of nanocellulosic 3D structures with high degree of control over morphology and versatility for tuning the properties and functionalities of the fabricated nanocellulosic objects opens up possibilities in various application fields, ranging from biomedical applications to in-water sensing systems.

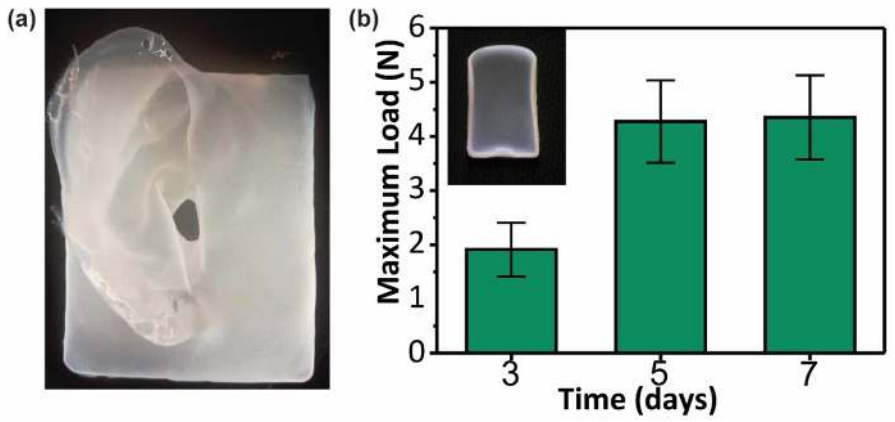

Figure 15. Production of 3D structures using superhydrophobized molds. (a) Ear shaped structure produced utilizing a superhydrophobized PLA mold. (b) Results of tensile tests with cuboid shaped objects produced using superhydrophobized polystyrene cuvettes as molds. (**Paper IV**)

5. Concluding Remarks and Prospects

In this thesis, nanocellulose was utilized to produce different types of architectures. Insights on the structure of these materials were achieved using different types of characterization techniques. They facilitated a better understanding on how the nanoscale structure of the materials translated into their properties. In **Paper I**, gelation occurred between phosphorylated CNF and uranium in a simple batch adsorption set-up, indicating the potential of phosphorylated CNF for use in uranium removal from water. In **Paper II**, granular composite materials containing cCNF with potential for water disinfection were produced by aqueous phase synthesis at room temperature. In **Papers III** and **IV**, BNC was produced in a 2D film form (**Paper III**) and as 3D structures using a new method (**Paper IV**). The application of these structures was studied for pressure-driven membrane separation in never-dried and dried state (**Paper III**) and for encapsulation of active molecules or particles (**Paper IV**). In all the production methods utilized in this thesis, the use of energy intensive drying processes, such as freeze-drying or critical point drying, and the extensive use of solvents and toxic chemicals was avoided. In **Papers III** and **IV**, no energy consuming mechanical treatments were applied to disintegrate the BNC structure since BNC was utilized in the as-grown state. Considering the advantages of the production processes used and the functionalities provided, these materials have potential for fulfilling the requirements for future materials for use in water treatment and other fields.

For potential implementation of the materials presented in this thesis in real-life applications, several future research directions are suggested. In the case of **Paper I**, additional studies would be beneficial to determine the removal efficiency from solutions with lower uranium concentrations. For **Paper II**, studies of the antibacterial efficiency in field samples would be suggested. For both **Paper I** and **II**, the potential to regenerate and reuse the materials should also be investigated. Comparison against commercial materials used for uranium removal and point-of use water disinfection, in terms of efficiency and cost, would also be suggested. For **Paper III**, studies to determine the molecular-weight cut-off and pore size distribution of the BNC membranes would complement the information on the filtration properties. In the case of **Paper IV**, opportunities provided by co-culturing of microorganisms or genetic engineering could be interesting directions to explore for expanding the application potential of the 3D biofabricated structures.

References

Abe, K. and Yano, H. (2011). Formation of hydrogels from cellulose nanofibers. *Carbohydrate Polymers*, 85(4), pp. 733-737. doi:10.1016/j.carbpol.2011.03.028.

Abouzeid, R. E. *et al.* (2019). Current State and New Trends in the Use of Cellulose Nanomaterials for Wastewater Treatment. *Biomacromolecules*, 20(2), pp. 573–597. doi: 10.1021/acs.biomac.8b00839.

Ajdary, R. *et al.* (2019). Acetylated Nanocellulose for Single-Component Bioinks and Cell Proliferation on 3D-Printed Scaffolds. *Biomacromolecules*, 20(7), pp. 2770–2778. doi: 10.1021/acs.biomac.9b00527.

Andrade, F. K. *et al.* (2013). Studies on the biocompatibility of bacterial nanocellulose. *Journal of Bioactive and Compatible Polymers*, 28(1), pp. 97–112. doi: 10.1177/0883911512467643.

Aussillous, P. and Quéré, D. (2001). Liquid marbles. *Nature*, 411(6840), pp. 924–927. doi: 10.1038/35082026.

Batmaz, R. *et al.* (2014). Cellulose nanocrystals as promising adsorbents for the removal of cationic dyes. *Cellulose*, 21(3), pp. 1655–1665. doi: 10.1007/s10570-014-0168-8.

Berto, S. *et al.* (2012). Advances in the investigation of dioxouranium (VI) complexes of interest for natural fluids. *Coordination Chemistry Reviews*, 256(1–2), pp. 63–81. doi: 10.1016/j.ccr.2011.08.015.

Bottan, S. *et al.* (2015). Surface-structured bacterial nanocellulose with guided assembly-based biolithography (GAB). *ACS Nano*, 9(1), pp. 206–219. doi: 10.1021/nn5036125.

Brown, A. J. (1886). XLIII.—On an acetic ferment which forms cellulose. *Journal of the Chemical Society, Transactions*, 49, pp. 432–439. doi: 10.1039/CT8864900432.

Carpenter, A. W., De Lannoy, C. F. and Wiesner, M. R. (2015). Cellulose nanomaterials in water treatment technologies. *Environmental Science and Technology*, 49(9), pp. 5277–5287. doi: 10.1021/es506351r.

Castro, C. *et al.* (2013). *Gluconacetobacter medellinensis* sp. nov., cellulose- and non-cellulose-producing acetic acid bacteria isolated from vinegar. *International Journal of Systematic and Evolutionary Microbiology*, 63(PART3), pp. 1119–1125. doi: 10.1099/ijs.0.043414-0.

Chaker, A. and Boufi, S. (2015). Cationic nanofibrillar cellulose with high antibacterial properties. *Carbohydrate Polymers*, 131, pp. 224–232. doi: 10.1016/j.carbpol.2015.06.003.

Chan, C. H. *et al.* (2015). Cellulose nanofibrils: A rapid adsorbent for the removal of methylene blue. *RSC Advances*, 5(24), pp. 18204–18212. doi: 10.1039/c4ra15754k.

Chen, L. and Peng, X. (2017). Silver nanoparticle decorated cellulose nanofibrous membrane with good antibacterial ability and high water permeability. *Applied Materials Today*, 9, pp. 130–135. doi: 10.1016/j.apmt.2017.06.005.

Chen, W. *et al.* (2014). Comparative study of aerogels obtained from differently prepared nanocellulose fibers. *ChemSusChem*, 7(1), pp. 154–161. doi: 10.1002/cssc.201300950.

Chen, W. *et al.* (2018). Nanocellulose: A promising nanomaterial for advanced electrochemical energy storage. *Chemical Society Reviews*, 47(8), pp. 2837–2872. doi: 10.1039/c7cs00790f.

Cheng, Q. *et al.* (2017). Facile fabrication of superhydrophilic membranes consisted of fibrous tunicate cellulose nanocrystals for highly efficient oil/water separation. *Journal of Membrane Science*, 525, pp. 1–8. doi: 10.1016/j.memsci.2016.11.084.

Chernousova, S. and Epple, M. (2013). Silver as antibacterial agent: Ion, nanoparticle, and metal. *Angewandte Chemie - International Edition*, 52(6), pp. 1636–1653. doi: 10.1002/anie.201205923.

Cruz-Tato, P. *et al.* (2017). Metalized Nanocellulose Composites as a Feasible Material for Membrane Supports: Design and Applications for Water Treatment. *Environmental Science and Technology*, 51(8), pp. 4585–4595. doi: 10.1021/acs.est.6b05955.

Czaja, W. K. *et al.* (2007). The future prospects of microbial cellulose in biomedical applications. *Biomacromolecules*, 8(1), pp. 1–12. doi: 10.1021/bm060620d.

Dong, X. M., Revol, J. F. and Gray, D. G. (1998). Effect of microcrystallite preparation conditions on the formation of colloid crystals of cellulose. *Cellulose*, 5(1), pp. 19–32. doi: 10.1023/A:1009260511939.

Dong, H., Snyder, James F, *et al.* (2013a). Hydrogel , aerogel and film of cellulose nanofibrils functionalized with silver nanoparticles. *Carbohydrate Polymers*, 95(2), pp. 760–767. doi: 10.1016/j.carbpol.2013.03.041.

Dong, H., Snyder, James F., *et al.* (2013b). Cation-induced hydrogels of cellulose nanofibrils with tunable moduli. *Biomacromolecules*, 14(9), pp. 3338–3345. doi: 10.1021/bm400993f.

Dubey, V. *et al.* (2002). Pervaporation of binary water-ethanol mixtures through bacterial nanocellulose membrane. *Separation and Purification Technology*, 27(2), pp. 163–171. doi: 10.1016/S1383-5866(01)00210-6.

Dufresne, A. and Paillet, M. (2002). Lignocellulosic flour-reinforced poly(hydroxybutyrate-co-valerate) composites. *Journal of Applied Polymer Science*, 87(8), pp. 1302-1315. doi: 10.1002/app.11546

Favier, V. *et al.* (1995). Nanocomposite materials from latex and cellulose whiskers. *Polymers for Advanced Technologies*, 6(5), pp. 351–355. doi: 10.1002/pat.1995.220060514.

Ferreira, F.V. et al. (2020). Porous nanocellulose gels and foams: Breakthrough status in the development of scaffolds for tissue engineering. *Materials Today*, 37, pp. 126-141. doi: 10.1016/j.mattod.2020.03.003.

De France, K. *et al.* (2020). Functional Materials from Nanocellulose: Utilizing Structure–Property Relationships in Bottom-Up Fabrication. *Advanced Materials*, 2000657. doi: 10.1002/adma.202000657.

Fu, L. *et al.* (2013). Evaluation of bacterial nanocellulose-based uniform wound dressing for large area skin transplantation. *Materials Science & Engineering C*, 33(5), pp. 2995–3000. doi: 10.1016/j.msec.2013.03.026.

Fukuzumi, H. *et al.* (2014). Dispersion stability and aggregation behavior of TEMPO-oxidized cellulose nanofibrils in water as a function of salt addition. *Cellulose*, 21(3), pp. 1553–1559. doi: 10.1007/s10570-014-0180-z.

Galdino, C. J. S. *et al.* (2020). Use of a bacterial nanocellulose filter for the removal of oil from wastewater. *Process Biochemistry*, 91, pp. 288–296. doi: 10.1016/j.procbio.2019.12.020.

da Gama, F. M. P. and Dourado, F. (2018). Bacterial nanocellulose: What future?. *BioImpacts*, 8(1), pp. 1–3. doi: 10.15171/bi.2018.01.

Geisel, N. *et al.* (2016). Microstructured Multilevel Bacterial nanocellulose Allows the Guided Growth of Neural Stem Cells. *Small*, 12(39), pp. 5407–5413. doi: 10.1002/smll.201601679.

Gelin, K. *et al.* (2007). Characterization of water in bacterial nanocellulose using dielectric spectroscopy and electron microscopy. *Polymer*, 48(26), pp. 7623–7631. doi: 10.1016/j.polymer.2007.10.039.

Ghanadpour, M. *et al.* (2015). Phosphorylated Cellulose Nanofibrils: A Renewable Nanomaterial for the Preparation of Intrinsically Flame-Retardant Materials. *Biomacromolecules*, 16(10), pp. 3399–3410. doi: 10.1021/acs.biomac.5b01117.

Gupta, P. *et al.* (2018). Low density and high strength nanofibrillated cellulose aerogel for thermal insulation application. *Materials and Design*, 158, pp. 224–236. doi: 10.1016/j.matdes.2018.08.031.

Gustafsson, S. and Mihranyan, A. (2016a). Strategies for Tailoring the Pore-Size Distribution of Virus Retention Filter Papers. *ACS Applied Materials and Interfaces*, 8(22), pp. 13759–13767. doi: 10.1021/acsami.6b03093.

Gustafsson, S. *et al.* (2016b). Mille-feuille paper: A novel type of filter architecture for advanced virus separation applications. *Materials Horizons*, 3(4), pp. 320–327. doi: 10.1039/c6mh00090h.

Habibi, Y. (2014). Key advances in the chemical modification of nanocelluloses. *Chemical Society Reviews*, 43(5), pp. 1519–1542. doi: 10.1039/c3cs60204d.

Håkansson, K. M. O. *et al.* (2016). Solidification of 3D Printed Nanofibril Hydrogels into Functional 3D Cellulose Structures. *Advanced Materials Technologies*, 1(7), pp. 1–9. doi: 10.1002/admt.201600096.

Hassan, E. *et al.* (2017). Use of Bacterial nanocellulose and Crosslinked Cellulose Nanofibers Membranes for Removal of Oil from Oil-in-Water Emulsions. Polymers, 9, 388. doi: 10.3390/polym9090388.

Heath, L. and Thielemans, W. (2010). Cellulose nanowhisker aerogels. *Green Chemistry*, 12(8), pp. 1448–1453. doi: 10.1039/c0gc00035c.

Henriksson, M. *et al.* (2007). An environmentally friendly method for enzyme-assisted preparation of microfibrillated cellulose (MFC) nanofibers. *European Polymer Journal*, 43(8), pp. 3434–3441. doi: 10.1016/j.eurpolymj.2007.05.038.

Henriksson, M. *et al.* (2008). Cellulose nanopaper structures of high toughness. *Biomacromolecules*, 9(6), pp. 1579–1585. doi: 10.1021/bm800038n.

Herrick, F.W. *et al.* (1983). Microfibrillated cellulose: morphology and accessibility. Journal of Applied Polymer Science: Appl. Polym. Symp., 37.

Hokkanen, S. *et al.* (2014). Adsorption of Ni(II), Cu(II) and Cd(II) from aqueous solutions by amino modified nanostructured microfibrillated cellulose. *Cellulose*, 21(3), pp. 1471–1487. doi: 10.1007/s10570-014-0240-4.

Hokkanen, S. *et al.* (2018). Removal of Cd^{2+}, Ni^{2+} and PO_4^{3-} from aqueous solution by hydroxyapatite-bentonite clay-nanocellulose composite. *International Journal of Biological Macromolecules*, 118, pp. 903–912. doi: 10.1016/j.ijbiomac.2018.06.095.

Hokkanen, S., Bhatnagar, A. and Sillanpää, M. (2016). A review on modification methods to cellulose-based adsorbents to improve adsorption capacity. *Water Research*, 91, pp. 156–173. doi: 10.1016/j.watres.2016.01.008.

Hokkanen, S., Repo, E. and Sillanpää, M. (2013). Removal of heavy metals from aqueous solutions by succinic anhydride modified mercerized nanocellulose. *Chemical Engineering Journal*, 223, pp. 40–47. doi: 10.1016/j.cej.2013.02.054.

Hou, Y. *et al.* (2019). Functional bacterial nanocellulose membranes with 3D porous architectures: Conventional drying, tunable wettability and water/oil separation. *Journal of Membrane Science*, 591, p. 117312. doi: 10.1016/j.memsci.2019.117312.

Hu, Y. and Catchmark, J. M. (2010). Formation and characterization of spherelike bacterial nanocellulose particles produced by *Acetobacter xylinum* JCM 9730 strain. *Biomacromolecules*, 11(7), pp. 1727–1734. doi: 10.1021/bm100060v.

Hüsing, N. and Schubert, U. (1998). Aerogels - Airy Materials: Chemistry, Structure, and Properties. *Angewandte Chemie - International Edition*, 37(1–2), pp. 22–45. doi: 10.1002/(SICI)1521-3773(19980202)37:1/23.0.CO;2-I.

Iguchi, M, Yamanaka S. and Budhiono, A. (2000). Bacterial nanocellulose — a masterpiece of nature 's arts. *Journal of Materials Science*, 35, pp. 261–270. doi: 10.1023/A:1004775229149

Iwamoto, S., Abe, K. and Yano, H. (2008). The effect of hemicelluloses on wood pulp nanofibrillation and nanofiber network characteristics. *Biomacromolecules*, 9(3), pp. 1022–1026. doi: 10.1021/bm701157n.

Jannasch, H. W. (1969). Estimations of Bacterial Growth Rates in Natural Waters. *Journal of Bacteriology*, 99(1), pp. 156–160.

Jiang, F. and Hsieh, Y. Lo (2014a). Super water absorbing and shape memory nanocellulose aerogels from TEMPO-oxidized cellulose nanofibrils via cyclic freezing-thawing. *Journal of Materials Chemistry A*, 2(2), pp. 350–359. doi: 10.1039/c3ta13629a.

Jiang, F. and Hsieh, Y. Lo (2014b). Amphiphilic superabsorbent cellulose nanofibril aerogels. *Journal of Materials Chemistry A*, 2(18), pp. 6337–6342. doi: 10.1039/c4ta00743c.

Jiang, F. and Hsieh, Y. Lo (2017). Cellulose nanofibril aerogels: Synergistic improvement of hydrophobicity, strength, and thermal stability via cross-linking with diisocyanate. *ACS Applied Materials and Interfaces*, 9(3), pp. 2825–2834. doi: 10.1021/acsami.6b13577.

Jiang, Q. *et al.* (2019). Photothermally Active Reduced Graphene Oxide/Bacterial nanocellulose Composites as Biofouling-Resistant Ultrafiltration Membranes. *Environmental Science and Technology*, 53(1), pp. 412–421. doi: 10.1021/acs.est.8b02772.

Karim, Z. *et al.* (2016). Nanocellulose based functional membranes for water cleaning : Tailoring of mechanical properties , porosity and metal ion capture. *Journal of Membrane Science*, 514, pp. 418–428. doi: 10.1016/j.memsci.2016.05.018.

Karim, Z. *et al.* (2017). In situ TEMPO surface functionalization of nanocellulose membranes for enhanced adsorption of metal ions from aqueous medium. *RSC Advances*, 7(9), pp. 5232–5241. doi: 10.1039/c6ra25707k.

Khan, M. H., Warwick, P. and Evans, N. (2006). Spectrophotometric determination of uranium with arsenazo-III in perchloric acid. *Chemosphere*, 63(7), pp. 1165-1169. doi: 10.1016/j.chemosphere.2005.09.060.

Klemm, D. *et al.* (2001). Bacterial synthesized cellulose-artificial blood vessels for microsurgery. Progress in Polymer Science, 26(9), pp. 1561-1603. doi: 10.1016/S0079-6700(01)00021-1.

Klemm, D. *et al.* (2005). Cellulose : Fascinating Biopolymer and Sustainable Raw Material. *Angewandte Chemie - International Edition*, 44(22), pp. 3358–3393. doi: 10.1002/anie.200460587.

Klemm, D. *et al.* (2011). Nanocelluloses : A New Family of Nature-Based Materials. *Angewandte Chemie - International Edition*, 50(24), pp. 5438–5466. doi: 10.1002/anie.201001273.

Klemm, D. *et al.* (2018). Nanocellulose as a natural source for groundbreaking applications in materials science : Today's state. *Materials Today*, 21(7), pp. 720–748. doi: 10.1016/j.mattod.2018.02.001.

Kobayashi, Y., Saito, T. and Isogai, A. (2014). Aerogels with 3D ordered nanofiber skeletons of liquid-crystalline nanocellulose derivatives as tough and transparent insulators. *Angewandte Chemie - International Edition*, 53(39), pp. 10394–10397. doi: 10.1002/anie.201405123.

Kong, L. *et al.* (2014). Superior effect of TEMPO-oxidized cellulose nanofibrils (TOCNs) on the performance of cellulose triacetate (CTA) ultrafiltration membrane. *Desalination*, 332(1), pp. 117–125. doi: 10.1016/j.desal.2013.11.005.

Kontturi, E. *et al.* (2018). Advanced Materials through Assembly of Nanocelluloses. *Advanced Materials*, 30(24). doi: 10.1002/adma.201703779.

Korhonen, J. T. *et al.* (2011). Hydrophobic nanocellulose aerogels as floating, sustainable, reusable, and recyclable oil absorbents. *ACS Applied Materials and Interfaces*, 3(6), pp. 1813–1816. doi: 10.1021/am200475b.

Lee, A., Elam, J. W. and Darling, S. B. (2016). Membrane materials for water purification: Design, development, and application. *Environmental Science: Water Research and Technology*, 2(1), pp. 17–42. doi: 10.1039/c5ew00159e.

Levard *et al.* (2013a). Effect of chloride on the dissolution rate of silver nanoparticles and toxicity to *E. coli*. *Environmental Science and Technology*, 47(11), pp. 5738–5745. doi: 10.1021/es400396f.

Levard *et al.* (2013b). Sulfidation of silver nanoparticles: Natural antidote to their toxicity. *Environmental Science and Technology*, 47(23), pp. 13440–13448. doi: 10.1021/es403527n.

Liimatainen, H. *et al.* (2013). Sulfonated cellulose nanofibrils obtained from wood pulp through regioselective oxidative bisulfite pre-treatment. *Cellulose*, 20(2), pp. 741–749. doi: 10.1007/s10570-013-9865-y.

Liu, A. *et al.* (2011). Clay nanopaper with tough cellulose nanofiber matrix for fire retardancy and gas barrier functions. *Biomacromolecules*, 12(3), pp. 633–641. doi: 10.1021/bm101296z.

Liu, P. *et al.* (2015). Nanocelluloses and their phosphorylated derivatives for selective adsorption of Ag^{+}, Cu^{2+} and Fe^{3+} from industrial effluents. *Journal of Hazardous Materials*, 294, pp. 177-185. doi: 10.1016/j.jhazmat.2015.04.001.

Liu, Y. *et al.* (2019). Assembly, Gelation, and Helicoidal Consolidation of Nanocellulose Dispersions. *Langmuir*, 35(10), pp. 3600–3606. doi: 10.1021/acs.langmuir.8b04013.

Lv, J. *et al.* (2018). Improvement of antifouling performances for modified PVDF ultrafiltration membrane with hydrophilic cellulose nanocrystal. *Applied Surface Science*, 440, pp. 1091–1100. doi: 10.1016/j.apsusc.2018.01.256.

Ma, H. *et al.* (2011). Ultrafine polysaccharide nanofibrous membranes for water purification. *Biomacromolecules*, 12(4), pp. 970–976. doi: 10.1021/bm1013316.

Ma, H., Hsiao, B. S. and Chu, B. (2012). Ultrafine Cellulose Nanofibers as Efficient Adsorbents for Removal of UO_2^{2+} in water. *ACS Macro Letters*, 1, pp. 213-216. doi: 10.1021/mz200047q

Ma, H. *et al.* (2014). Fabrication and characterization of cellulose nanofiber based thin-film nanofibrous composite membranes. *Journal of Membrane Science*, 454, pp. 272–282. doi: 10.1016/j.memsci.2013.11.055.

Mautner, A. *et al.* (2014). Nanopapers for organic solvent nanofiltration. *Chemical Communications*, 50(43), pp. 5778–5781. doi: 10.1039/c4cc00467a.

Mautner, A. *et al.* (2015). Cellulose nanopapers as tight aqueous ultra-filtration membranes. *Reactive and Functional Polymers*, 86, pp. 209–214. doi: 10.1016/j.reactfunctpolym.2014.09.014.

Mautner, A. *et al.* (2016). Phosphorylated nanocellulose papers for copper adsorption from aqueous solutions. *International Journal of Environmental Science and Technology*, 13(8), pp. 1861–1872. doi: 10.1007/s13762-016-1026-z.

Mekonnen, M. M. and Hoekstra, A. Y. (2016). Sustainability: Four billion people facing severe water scarcity. *Science Advances*, 2(2), pp. 1–7. doi: 10.1126/sciadv.1500323.

Mendoza, L. *et al.* (2018). Gelation mechanism of cellulose nanofibre gels: A colloids and interfacial perspective. *Journal of Colloid and Interface Science*, 509, pp. 39–46. doi: 10.1016/j.jcis.2017.08.101.

Metreveli, G. *et al.* (2014). A Size-Exclusion Nanocellulose Filter Paper for Virus Removal. *Advanced Healthcare Materials*, 3(10), pp. 1546–1550. doi: 10.1002/adhm.201300641.

Moon, R. J. *et al.* (2011). Cellulose nanomaterials review: Structure, properties and nanocomposites. *Chemical Society Reviews*, 40, pp. 3941-3994. doi: 10.1039/c0cs00108b.

Moreira, S. *et al.* (2009). BNC nanofibres: In vitro study of genotoxicity and cell proliferation. *Toxicology Letters*, 189(3), pp. 235–241. doi: 10.1016/j.toxlet.2009.06.849.

Nagar, A. and Pradeep, T. (2020). Clean Water through Nanotechnology: Needs, Gaps, and Fulfillment. *ACS Nano*, 14(6), pp. 6420-6435. doi: 10.1021/acsnano.9b01730.

Neumann, O. *et al.* (2013). Solar Vapor Generation Enabled by Nanoparticles. *ACS Nano,* 7(1), pp. 42-49. doi: 10.1021/nn304948h.

Nguyen, P. Q. *et al.* (2018). Engineered Living Materials: Prospects and Challenges for Using Biological Systems to Direct the Assembly of Smart Materials. *Advanced Materials*, 30(19), pp. 1–34. doi: 10.1002/adma.201704847.

Nimeskern, L. *et al.* (2013). Mechanical evaluation of bacterial nanocellulose as an implant material for ear cartilage replacement. *Journal of the Mechanical Behavior of Biomedical Materials*, 22, pp. 12–21. doi: 10.1016/j.jmbbm.2013.03.005.

Nunes, S. P. *et al.* (2020). Thinking the future of membranes: Perspectives for advanced and new membrane materials and manufacturing processes. *Journal of Membrane Science*, 598, p. 117761. doi: 10.1016/j.memsci.2019.117761.

Olsson, R. T. *et al.* (2010). Making flexible magnetic aerogels and stiff magnetic nanopaper using cellulose nanofibrils as templates. *Nature Nanotechnology*, 5(8), pp. 584–588. doi: 10.1038/nnano.2010.155.

Olszewska, A. *et al.* (2011). The behaviour of cationic NanoFibrillar Cellulose in aqueous media. *Cellulose*, 18(5), pp. 1213–1226. doi: 10.1007/s10570-011-9577-0.

Orelma, H. *et al.* (2014). Affibody conjugation onto bacterial nanocellulose tubes and bioseparation of human serum albumin. *RSC Advances*, 4(93), pp. 51440–51450. doi: 10.1039/c4ra08882d.

Oshima, T. *et al.* (2008). Preparation of phosphorylated bacterial nanocellulose as an adsorbent for metal ions. *Reactive and Functional Polymers*, 68(1), pp. 376–383. doi: 10.1016/j.reactfunctpolym.2007.07.046.

Pääkkö, M. *et al.* (2007). Enzymatic hydrolysis combined with mechanical shearing and high-pressure homogenization for nanoscale cellulose fibrils and strong gels. *Biomacromolecules*, 8(6), pp. 1934–1941. doi: 10.1021/bm061215p.

Pääkkö, M. *et al.* (2008). Long and entangled native cellulose i nanofibers allow flexible aerogels and hierarchically porous templates for functionalities. *Soft Matter*, 4(12), pp. 2492–2499. doi: 10.1039/b810371b.

Pandey, L. K., Saxena, C. and Dubey, V. (2005). Studies on pervaporative characteristics of bacterial nanocellulose membrane. *Separation and Purification Technology*, 42(3), pp. 213–218. doi: 10.1016/j.seppur.2004.07.014.

Pradeep, T. and Anshup (2009). Noble metal nanoparticles for water purification: A critical review. *Thin Solid Films*, 517(24), pp. 6441–6478. doi: 10.1016/j.tsf.2009.03.195.

Prodromou M. and Pashalidis I. (2013). Uranium adsorption by non-treated and chemically modified cactus fibres in aqueous solutions. *Journal of Radioanalytical and Nuclear Chemistry*, 298, pp. 1587–1595. 10.1007/s10967-013-2565-0.

Putra, A. *et al.* (2008). Tubular bacterial nanocellulose gel with oriented fibrils on the curved surface. *Polymer*, 49(7), pp. 1885–1891. doi: 10.1016/j.polymer.2008.02.022.

Quellmalz, A. and Mihranyan, A. (2015). Citric Acid Cross-Linked Nanocellulose-Based Paper for Size-Exclusion Nanofiltration. *ACS Biomaterials Science and Engineering*, 1(4), pp. 271–276. doi: 10.1021/ab500161x.

Rajala, S. *et al.* (2016). Cellulose Nanofibril Film as a Piezoelectric Sensor Material. *ACS Applied Materials and Interfaces*, 8(24), pp. 15607-15614. doi: 10.1021/acsami.6b03597.

Rathod, M., Haldar, S. and Basha, S. (2015). Nanocrystalline cellulose for removal of tetracycline hydrochloride from water via biosorption: Equilibrium, kinetic and thermodynamic studies. *Ecological Engineering*, 84, pp. 240–249. doi: 10.1016/j.ecoleng.2015.09.031.

Ross, P., Mayer, R. and Benziman, M. (1991). Cellulose biosynthesis and function in bacteria. *Microbiological Reviews*, 55(1), pp. 35–58. doi: 10.1128/mmbr.55.1.35-58.1991.

Rühs, P. A. *et al.* (2018). 3D bacterial nanocellulose biofilms formed by foam templating. *npj Biofilms and Microbiomes*, 4(1), pp. 1–6. doi: 10.1038/s41522-018-0064-3.

Sacui, I. A. *et al.* (2014). Comparison of the properties of cellulose nanocrystals and cellulose nanofibrils isolated from bacteria, tunicate, and wood processed using acid, enzymatic, mechanical, and oxidative methods. *ACS Applied Materials and Interfaces*, 6(9), pp. 6127–6138. doi: 10.1021/am500359f.

Saito, T. *et al.* (2007). Cellulose nanofibers prepared by TEMPO-mediated oxidation of native cellulose. *Biomacromolecules*, 8(8), pp. 2485–2491. doi: 10.1021/bm0703970.

Saito, T. *et al.* (2011). Self-aligned integration of native cellulose nanofibrils towards producing diverse bulk materials. *Soft Matter*, 7(19), pp. 8804–8809. doi: 10.1039/c1sm06050c.

Saito, T. *et al.* (2013). An ultrastrong nanofibrillar biomaterial: The strength of single cellulose nanofibrils revealed via sonication-induced fragmentation. *Biomacromolecules*, 14(1), pp. 248–253. doi: 10.1021/bm301674e.

Sankar, M. U. *et al.* (2013). Biopolymer-reinforced synthetic granular nanocomposites for affordable point-of-use water purification. *Proceedings of the National Academy of Sciences*, 110(21), pp. 8459–8464. doi: 10.1073/pnas.1220222110.

Schaffner, M. *et al.* (2017). 3D printing of bacteria into functional complex materials. *Science Advances*, 3(12). doi: 10.1126/sciadv.aao6804.

Schmitt, J. *et al.* (2018). TEMPO-oxidised cellulose nanofibrils; Probing the mechanisms of gelation: Via small angle X-ray scattering. *Physical Chemistry Chemical Physics*, 20(23), pp. 16012–16020. doi: 10.1039/c8cp00355f.

Sehaqui, H. *et al.* (2010). Mechanical performance tailoring of tough ultra-high porosity foams prepared from cellulose I nanofiber suspensions. *Soft Matter*, 6(8), pp. 1824–1832. doi: 10.1039/b927505c.

Sehaqui, H. *et al.* (2011). Strong and tough cellulose nanopaper with high specific surface area and porosity. *Biomacromolecules*, 12(10), pp. 3638–3644. doi: 10.1021/bm2008907.

Sehaqui, H. *et al.* (2014). Enhancing adsorption of heavy metal ions onto biobased nanofibers from waste pulp residues for application in wastewater treatment. *Cellulose*, 21(4), pp. 2831–2844. doi: 10.1007/s10570-014-0310-7.

Sehaqui, H., *et al.* (2016a). Cationic cellulose nanofibers from waste pulp residues and their nitrate, fluoride, sulphate and phosphate adsorption properties. *Carbohydrate Polymers*, 135, pp. 334–340. doi: 10.1016/j.carbpol.2015.08.091.

Sehaqui, H., *et al.* (2016b). Functional cellulose nanofiber filters with enhanced flux for the removal of humic acid by adsorption. *ACS Sustainable Chemistry and Engineering*, 4(9), pp. 4582–4590. doi: 10.1021/acssuschemeng.6b00698.

Sharma P.R., *et al.* (2017). Efficient removal of UO_2^{2+} from water using carboxycellulose nanofibers prepared by the nitro-oxidation method. *Industrial and Engineering Chemistry Research*, 56, pp. 13885–13893. 10.1021/acs.iecr.7b03659

Sharma, P. R. *et al.* (2020). Nanocellulose-Enabled Membranes for Water Purification: Perspectives. *Advanced Sustainable Systems*, 4(5), pp. 1–28. doi: 10.1002/adsu.201900114.

Shen, W. *et al.* (2009). Adsorption of Cu(II) and Pb(II) onto diethylenetriamine-bacterial nanocellulose. *Carbohydrate Polymers*, 75(1), pp. 110–114. doi: 10.1016/j.carbpol.2008.07.006.

Shin, S. *et al.* (2019). Solid matrix-assisted printing for three-dimensional structuring of a viscoelastic medium surface. *Nature Communications*, 10(1). doi: 10.1038/s41467-019-12585-9.

Singh, K., Sinha, T. J. M. and Srivastava, S. (2015). Functionalized nanocrystalline cellulose: Smart biosorbent for decontamination of arsenic. *International Journal of Mineral Processing*, 139, pp. 51–63. doi: 10.1016/j.minpro.2015.04.014.

Siró, I. and Plackett, D. (2010). Microfibrillated cellulose and new nanocomposite materials: A review. *Cellulose*, 17(3), pp. 459–494. doi: 10.1007/s10570-010-9405-y.

Soyekwo, F. *et al.* (2016). Facile preparation and separation performances of cellulose nanofibrous membranes. *Journal of Applied Polymer Science*, 133(24), pp. 1–12. doi: 10.1002/app.43544.

Stelte, W. and Sanadi, A. R. (2009). Preparation and characterization of cellulose nanofibers from two commercial hardwood and softwood pulps. *Industrial and Engineering Chemistry Research*, 48(24), pp. 11211–11219. doi: 10.1021/ie9011672.

Sultan, S. *et al.* (2017). 3D printing of nano-cellulosic biomaterials for medical applications. *Current Opinion in Biomedical Engineering*, 2, pp. 29–34. doi: 10.1016/j.cobme.2017.06.002.

Suman *et al.* (2015). A novel reusable nanocomposite for complete removal of dyes, heavy metals and microbial load from water based on nanocellulose and silver nano-embedded pebbles. *Environmental Technology (United Kingdom)*, 36(6), pp. 706–714. doi: 10.1080/09593330.2014.959066.

Suopajärvi, T. *et al.* (2015). Lead adsorption with sulfonated wheat pulp nanocelluloses. *Journal of Water Process Engineering*, 5, pp. 136–142. doi: 10.1016/j.jwpe.2014.06.003.

Swathy, J. R. *et al.* (2014). Antimicrobial silver: An unprecedented anion effect. *Scientific Reports*, 11. doi: 10.1038/srep07161.

Sylwester, E., Hudson, E. and Allen, P. (2000). The structure of uranium (VI) sorption complexes on silica, alumina, and montmorillonite. *Geochimica et Cosmochimica Acta*, 64(14), pp. 2431–2438. doi: 10.1016/S0016-7037(00)00376-8.

Tian, J. *et al.* (2013). Respirable liquid marble for the cultivation of microorganisms. *Colloids and Surfaces B: Biointerfaces*, 106, pp. 187–190. doi: 10.1016/j.colsurfb.2013.01.016.

Turbak A.F., Snyder F.W. and Sandberg K.R. (1983). Microfibrillated cellulose, a new cellulose product: properties, uses, and commercial potential. Journal of Applied Polymer Science: Appl. Polym. Symp. 37.

U.S. Environmental Protection Agency (2012). 2012 Edition of the Drinking Water Standards and Health Advisories 2012 Edition of the Drinking Water Standards and Health Advisories.

Ul-islam, M., Khan, T. and Park, K. J. (2012). Water holding and release properties of bacterial nanocellulose obtained by in situ and ex situ modification. *Carbohydrate Polymers*, 88(2), pp. 596–603. doi: 10.1016/j.carbpol.2012.01.006.

Varanasi, S., Low, Z. X. and Batchelor, W. (2015). Cellulose nanofibre composite membranes - Biodegradable and recyclable UF membranes. *Chemical Engineering Journal*, 265(1), pp. 138–146. doi: 10.1016/j.cej.2014.11.085.

Visanko, M. *et al.* (2014). Porous thin film barrier layers from 2,3-dicarboxylic acid cellulose nanofibrils for membrane structures. *Carbohydrate Polymers*, 102(1), pp. 584–589. doi: 10.1016/j.carbpol.2013.12.006.

Voisin, H. *et al.* (2017). Nanocellulose-based materials for water purification. *Nanomaterials*, 7(3). doi: 10.3390/nano7030057.

Wågberg, L. *et al.* (2008). The build-up of polyelectrolyte multilayers of microfibrillated cellulose and cationic polyelectrolytes. *Langmuir*, 24(3), pp. 784–795. doi: 10.1021/la702481v.

Wang, R. *et al.* (2013). Nanofibrous microfiltration membranes capable of removing bacteria, viruses and heavy metal ions. *Journal of Membrane Science*, 446, pp. 376–382. doi: 10.1016/j.memsci.2013.06.020.

Wang, J. J. *et al.* (2017a). Nanofiltration membranes with cellulose nanocrystals as an interlayer for unprecedented performance. *Journal of Materials Chemistry A*, 5(31), pp. 16289–16295. doi: 10.1039/c7ta00501f.

Wang, D. C. *et al.* (2017b). Superfast Adsorption-Disinfection Cryogels Decorated with Cellulose Nanocrystal/Zinc Oxide Nanorod Clusters for Water-Purifying Microdevices. *ACS Sustainable Chemistry and Engineering*, 5(8), pp. 6776–6785. doi: 10.1021/acssuschemeng.7b01029.

Wang, Z. *et al.* (2019). Preparation of nanocellulose/filter paper (NC/FP) composite membranes for high-performance filtration. *Cellulose*, 26(2), pp. 1183–1194. doi: 10.1007/s10570-018-2121-8.

Wu, C. N. *et al.* (2012). Ultrastrong and high gas-barrier nanocellulose/clay-layered composites. *Biomacromolecules*, 13(6), pp. 1927–1932. doi: 10.1021/bm300465d.

Xie, Y. *et al.* (2019). Progress in Materials Science Emerging natural and tailored materials for uranium-contaminated water treatment and environmental remediation. *Progress in Materials Science*, 103, pp. 180–234. doi: 10.1016/j.pmatsci.2019.01.005.

Xing, J. *et al.* (2019). Nanocellulose-graphene composites: A promising nanomaterial for flexible supercapacitors. *Carbohydrate Polymers*, 207, pp. 447–459. doi: 10.1016/j.carbpol.2018.12.010.

Xu, T. *et al.* (2018). Catalytically Active Bacterial nanocellulose-Based Ultrafiltration Membrane. *Small*, 14(15), pp. 1–8. doi: 10.1002/smll.201704006.

Yamanaka, S. *et al.* (1989). The structure and mechanical properties of sheets prepared from bacterial nanocellulose. *Journal of Materials Science*, 24(9), pp. 3141–3145. doi: 10.1007/BF01139032.

Yu, X. *et al.* (2013). Adsorption of heavy metal ions from aqueous solution by carboxylated cellulose nanocrystals. *Journal of Environmental Sciences (China)*, 25(5), pp. 933–943. doi: 10.1016/S1001-0742(12)60145-4.

Zhang, W. *et al.* (2012). Aerogels from crosslinked cellulose nano/micro-fibrils and their fast shape recovery property in water. *Journal of Materials Chemistry*, 22(23), pp. 11642–11650. doi: 10.1039/c2jm30688c.

Zhang, X. *et al.* (2014a). Acrylic acid grafted and acrylic acid/sodium humate grafted bamboo cellulose nanofibers for Cu^{2+} adsorption. *RSC Advances*, 4(98), pp. 55195–55201. doi: 10.1039/c4ra08307e.

Zhang, Z. *et al.* (2014b). Ultralightweight and flexible silylated nanocellulose sponges for the selective removal of oil from water. *Chemistry of Materials*, 26(8), pp. 2659–2668. doi: 10.1021/cm5004164.

Zhu, H. *et al.* (2011). Preparation and application of bacterial nanocellulose sphere: A novel biomaterial. *Biotechnology and Biotechnological Equipment*, 25(1), pp. 2233–2236. doi: 10.5504/bbeq.2011.0010.

Zu, G. *et al.* (2016). Nanocellulose-derived highly porous carbon aerogels for supercapacitors, *Carbon*., 99, pp. 203–211. doi: 10.1016/j.carbon.2015.11.079.

Aalto-DD 218/2020

ISBN 978-952-64-0202-4 (printed)
ISBN 978-952-64-0203-1 (pdf)
ISSN 1799-4934 (printed)
ISSN 1799-4942 (pdf)

Aalto University
School of Chemical Engineering
Department of Bioproducts and Biosystems
www.aalto.fi

BUSINESS + ECONOMY

ART + DESIGN + ARCHITECTURE

SCIENCE + TECHNOLOGY

CROSSOVER

DOCTORAL DISSERTATIONS